ABSTRACT

Title of dissertation: MULTIDIMENSIONAL PROTEIN SEPARATIONS IN A PLASTIC MICROFLUIDIC NETWORK

Yan Li, Doctor of Philosophy, 2003

Dissertation directed by: Professor Cheng S. Lee
Department of Chemistry and Biochemistry

The field of microfabrication of bioanalytical devices has grown significantly over the last decade from academic research to several commercially available systems. The performances of the microfluidic systems in terms of reproducibility, resolution, sensitivity, and speed can be achieved by applying these technologies to complex biological samples.

A commonly used capillary fitting is employed for housing miniaturized membrane chromatography for performing reversed-phase peptide separations. Separation performance of cytochrome C digest in miniaturized membrane chromatography is compared with the results obtained from μ-LC and capillary LC. The use of miniaturized membrane chromatography allows significant reduction in sample consumption together with enhanced detection sensitivity.

In order to further reduce sample consumption and dead volume, an isoelectric focusing separation and dynamic sample introduction are demonstrated in a microfluidic microchannel. The dynamic sample introduction in plastic microfluidic devices can be directly controlled by various electrokinetic conditions, including the injection time and

the applied electric field strength. It enhances sample loading and therefore the concentrations of focused analytes by approximately 10-100 fold in comparison with conventional isoelectric focusing.

An integrated 2-D protein separation system provides significant resolving power for complex protein mixtures. Non-native IEF is chosen for the first separation dimension and gel electrophoresis for the second dimension. Once the focusing is complete, the focusing proteins at IEF microchannel are simultaneously transferred using an electrokinetic method from the first dimensional microchannel into an array of the second dimensional microchannels for achieving parallel size-depended separation on each sampled fraction. Although this simple study involves a limited number of second dimensional microchannels, the ability for a microfluidic platform to perform parallel 2-D separations of complex protein samples has been successfully demonstrated.

This study investigates that microfabricated systems have the potential to automate and combine high throughput multidimensional protein separations in a microfluidic network. It is crucial to combine various microfluidic components, which enable all required proteome technologies in an integrated platform for a true lab-on-a-chip.

MULTIDIMENSIONAL PROTEIN SEPARATIONS IN A PLASTIC MICROFLUIDIC NETWORK

By

Yan Li

Dissertation submitted to the Faculty of the Graduate School of the
University of Maryland, College Park in partial fulfillment
of the requirements for the degree of
Doctor of Philosophy
2003

Advisory Committee:

Professor Cheng S. Lee, Chair
Professor Catherine C. Fenselau
Professor Janice E. Reutt-Robey
Professor Douglas English
Professor Stephen M. Mount

TABLE OF CONTENTS

LIST OF FIGURES ..... **ii**
LIST OF TABLES ..... **iii**

CHAPTER 1 MICROFLUIDICS-BASED PROTEOME ANALYSIS **1**
1.1 INTRODUCTION TO MICROFLUIDICS 1
1.2 MICROFLUIDICS-BASED PROTEIN/PEPTIDE SEPARATIONS 6
1.3 PROJECT DESCRIPTION 13

CHAPTER 2 FUNDAMENTAL THEORIES **16**
2.1 AMINO ACID AND PROTEINS 16
2.2 ISOELECTRIC FOCUSING SEPARATIONS 30
2.3 MICROFLUIDICS-BASED FIELD GRADIENT FOCUSING TECHNIQUES 36

CHAPTER 3 MINIATURIZED MEMBRANE-BASED REVERSED-PHASE CHROMATOGRAPHY AND ENZYME REACTOR FOR PROTEIN DIGESTION, PEPTIDE SEPARATION, AND PROTEIN IDENTIFICATION USING ESI-MS **38**
3.1 INTRODUCTION 38
3.2 EXPERIMENTAL 40
3.3 RESULTS AND DISCUSSION 44
3.4 CONCLUSION 52

CHAPTER 4 DYNAMIC ANALYTE INTRODUCTION AND FOCUSING IN PLASTIC MICROFLUIDIC DEVICES FOR PROTEOMIC ANALYSIS **53**
4.1 INTRODUCTION 53
4.2 MATERIALS AND METHODS 55
4.3 RESULTS AND DISCUSSION 58
4.4 CONCLUDING REMARKS 69

CHAPTER 5 INTEGRATION OF ISOELECTRIC FOCUSING WITH PARALLEL SDS GEL ELECTROPHORESIS FOR MULTIDIMENSIONAL PROTEIN SEPARATIONS IN A PLASTIC MICROFLUIDIC NETWORK **71**
5.1 INTRODUCTION 71
5.2 EXPERIMENTAL SECTION 74
5.3 RESULTS AND DISCUSSION 80
5.4 CONCLUSION 90

CHAPTER 6 CONCLUSION **92**
APPENDICES **96**
REFERENCES **97**

LIST OF FIGURES

Figure 2-1 17
Figure 2-3 23
Figure 2-4 26
Figure 2-5 27
Figure 2-6 29
Figure 3-1 41
Figure 3-2 42
Figure 3-3. 47
Figure 3-4. 51
Figure 3-5 51
Figure 4-1 61
Figure 4-2 64
Figure 4-3 66
Figure 4-4 68
Figure 5-1 77
Figure 5-2 82
Figure 5-3 84
Figure 5-4 87
Figure 5-5 88
Figure 5-6 89

LIST OF TABLES

Table 2-1 21
Table 4-1 62
Table 5-1 75

CHAPTER 1

MICROFLUIDICS-BASED PROTEOME ANALYSIS

1.1 INTRODUCTION TO MICROFLUIDICS

Since the concept of Micro-Total Analysis Systems (μTAS) was first proposed [1], the field has advanced rapidly, with ongoing developments promising to profoundly revolutionize modern bioanalytical methodologies. Whether termed μTAS, lab-on-a-chip, or microfluidics, the collection of technologies which define the field are proving to be an important innovation capable of transforming the ways in which bioanalytical techniques are performed. In particular, miniaturized bioanalytical devices based on microfluidics technology provide various important advantages over bench-top instruments.

The very act of miniaturization provides significant benefits for many microfluidic instruments. Reduced size and power requirements lead to improved portability, with higher levels of integration possible. Microfabrication methods lend themselves to the formation of complex microfluidic systems, opening the way to highly parallel analytical tools, while realizing low per-unit cost for disposable applications. Furthermore, the low volume fluid control enabled by microfluidics allows smaller dead volume and reduced sample consumption, while the low Reynolds numbers which characterize most microfluidic systems lead to highly laminar flow, eliminating the need for considering turbulent effects during instrument design. Many efficient pumping methods, including capillary action and electroosmotic flow, scale favorably in these systems, enabling valveless flow control at the microscale. Similarly, thermal time constants tend to be extremely small due to the large surface area to volume ratio,

reducing the onset of significant Joule heating during electrokinetic separations and thus allowing higher separation voltages for shorter analysis times and equivalent or better separation resolution for complex mixtures in an integrated format.

Choices of material and fabrication procedure are critical aspects of microfluidic devices. Currently, the majority of commercial devices are made from glass or silicon. In some cases, these materials are chosen for their inherent properties, for example the use of established methods for silica surfaces. However, these materials are often chosen in order to readily leverage established fabrication procedures from the semiconductor and microelectromechanical systems industries. For a wide range of applications, glass and silicon microfluidic devices suffer from high fabrication costs and poor mechanical robustness due to their brittle nature, leading to a demand for alternative substrate materials for commercial applications. To this end, plastics offer a very promising solution, enjoying advantages including lower cost, a wide range of surface properties, and ease of manufacture. One salient advantage is that plastic microfluidic systems are readily fabricated using replication techniques such as casting, embossing, or injection molding [2].

For example, the use of bulk-micromachined silicon templates containing raised three-dimensional patterns for imprinting microchannels into plastic substrates by hot embossing has been widely demonstrated [3]. By taking advantage of anisotropic silicon etching, in which the <111> family of crystal planes dictates the final geometry of silicon template features, well-defined microchannel molds may be realized with sidewalls sloped at 54.7^{o} from vertical. Alternately, deep reactive-ion etching of silicon may be used to form templates with nearly vertical sidewalls. This imprinting technique,

however, requires heating to soften the plastic near its glass transition temperature, enabling pattern transfer from the silicon template during imprinting. While effective, the disadvantage is that the silicon templates tend to break upon cooling due to mismatched thermal expansion coefficients between the silicon template and plastic substrate. In practice, a typical 100 mm diameter silicon template can only be used to imprint on the order of 10 devices before template failure occurs. More recently, a room temperature imprinting method for the fabrication of plastic microfluidic devices has been reported [4]. Since no external heating is involved, a single silicon template can be used to imprint scores of microdevices without concern for thermal mismatch failures. Furthermore, overall fabrication time per device is shortened from about 30 min to 5 min.

Templates based on electroplated metals, rather than silicon, are capable of producing embossing templates with features as small as several microns. Fabricated by electroplating thick metal films around a lithographically-defined polymer features (photoresist in the case of photolithographic patterning, or poly(methyl methacrylate) (PMMA) in the case of x-ray lithography), these templates are more difficult to manufacture than silicon devices but offer several key advantages. By eliminating silicon as the mold material, the electroplating process results in templates with significantly longer lifetimes, even when using higher temperature embossing conditions. In addition, the templates are produced with vertical microchannel walls, rather than sloped 54.7^{o} sidewalls produced by bulk etching of single crystal silicon. This allows both greater precision and flexibility in channel geometry, and reduces variations in electric field distribution across the channel cross section for improved uniformity during on-chip electrokinetic separations.

A wide range of rigid plastics have been used for microfluidic systems, including PMMA, poly(carbonate) (PC), poly(ethylene terephthalate) (PET), poly(ethyl ethylketone) (PEEK), and poly(vinylidenfluoride) (PVDF), to name only a few. Each of these materials offers different benefits in terms of chemical, mechanical, thermal, and optical properties. PC, for example, offers particular advantages in terms of excellent thermal and mechanical stability, high UV transmission for optical detection, and repeatable fabrication by injection molding or hot embossing, with dimensions of imprinted microchannels typically varying by less than 2% in height and width. Irreversible thermal sealing of polycarbonate microchannels has been demonstrated with bond energies equal to the native surface energy of bulk PC [5].

Another popular method for microfluidic fabrication is based on curing a silicone elastomeric material, such as poly(dimethylsiloxane) (PDMS), on a rigid mold to transfer the mold features into the elastomer. This method has been shown to successfully reproduce features with a 50 nm resolution [6], and has been extensively used for prototyping microfluidic systems. Permanent bonding of PDMS to a variety of rigid substrates to seal the microchannels is often achieved by pretreating PDMS with oxygen plasma. The plasma introduces silanol groups (Si-OH) at the expense of methyl groups (Si-CH3) [7,8] which condense with appropriate groups (OH, COOH, ketone) on another surface when the two layers are brought into conformal contact. Oxidized PDMS also seals irreversibly to other materials, including glass, silicon, silicon dioxide, quartz, silicon nitride, poly(ethylene), poly(styrene), and glassy carbon. Oxidation of the PDMS has the additional advantage that it renders the surface hydrophilic because of the presence of silanol groups. These negatively charged channels have greater resistance to

adsorption of hydrophobic and negatively charged analytes, and are capable of creating strong bond energies over twice the native PDMS surface energy, and comparable to the surface energy of rigid polymers such as PC.

Despite the benefits of PDMS fabrication methods, the material suffers from several key drawbacks. PDMS exhibits a high permeability for both gasses and, in some cases, analytes. It suffers from poor mechanical properties including low elastic modulus and low tensile strength which can lead to poor mechanical robustness and low geometric stability. Its low stiffness can also lead to difficulties with structural collapse when forming large open channels, chambers, and reservoirs. The ionic nature of the siloxane backbone in PDMS makes it susceptible to hydrolysis, and long-term exposure to water is capable of breaking the siloxane bond, especially at a pH lower than 2.5 or higher than 11. It is well known that PDMS suffers from limited life span for devices requiring stable surface charge for electroosmotic flow, and in general possesses low solvent stability. Thus, while PDMS offers a simple and attractive approach for microfluidic fabrication, it may not be suitable for all situations, particularly when a wide range of pH levels or long-term exposure to solution is required as in many proteomic applications.

1.2 MICROFLUIDICS-BASED PROTEIN/PEPTIDE SEPARATIONS

Different microfluidic systems have been applied to achieve protein/peptide separations as the essential aspects of the proteomics process. This session describes the promising proof-of-principle microfabricated devices which have been employed to perform chromatographic- or electrokinetic-based separations. Furthermore, recent developments of multidimensional protein/peptide separations in microfluidic network are critically needed, particularly for the analysis of complex protein mixtures such as cell lysates.

Shrinking Liquid Chromatography Landscape

The trend toward increasingly smaller columns and stationary phase structures in liquid chromatography can be accommodated by miniaturizing liquid phase separations in microfluidic network. Even though microchannels can be micromachined and packed with particles [9,10], substantial concerns, including the fabrication of frits, the nonuniformity of packing at the walls and corners of the channels, and the difficulty of packing columns through the tortuous channel network, still remain in on-chip liquid chromatography.

Open tubular columns with the stationary phase supported on the channel walls provide potential solution to circumvent the use of particles and the accompanying packing problems. Thus, microscale monolith arrays were fabricated on quartz substrates using dry reactive-ion etching [11]. In order to prepare the array for performing chromatography in reversed-phase mode, the surface of the array was coated with poly(styrene sulfonate) following surface derivatization with (γ-aminopropyl)-

trimethoxysilane. The monolith array was designed to act as flow splitters for enhanced interaction between the stationary phase and the chemical species in the mobile phase.

Additionally, photolithographically-patterned rigid polymer monoliths have been fabricated within the microchannels by Throckmorton and co-workers and employed to achieve reversed-phase separation of amino acids and peptides [12]. Still, the fabrication of high-efficiency stationary phase remains the toughest part in chip-based liquid chromatography systems [13]. Miniaturized chromatography separations have to be competitive with most of lab-on-a-chip technologies that are electrophoretically-based.

Electrokinetic-Based Separations

The use of chromatography far outweighs that of electrophoresis in analytical and microscale separations. However, the opposite is true for chip-based separations at the current stage. Besides difficulties involved in the fabrication and the packing of stationary phase for miniaturized chromatography, it is easier to apply a high voltage to a chip than pressure. Owing to its simplicity of implementation, zone electrophoresis remains the most popular method among miniaturized electrokinetic-based techniques [14]. Under the influence of electric potential applied across the buffer-filled microchannels, the charged surface on the channel wall offers an electrically-driven pump, the electroosmotic flow. The presence of electroosmotic pumping, the bulk flow of liquid, facilitates the zone resolution of neutral, cationic, or anionic analytes and mobilizes all the analytes toward the same direction in the channel for detection.

Efforts including the manipulation of buffer conditions [15] and the use of surface modifications [16], however, are needed to eliminate or significantly reduce any surface-

analyte interactions. The adsorption of protein/peptide onto the channel wall not only degrades the separation efficiency, but also can cause irreversible loss of analytes. Furthermore, sample loading is already a critical issue for capillary electrophoresis and even more seriously for on-chip zone electrophoresis with limited injection volume. Thus, various sample pre-concentration strategies, including sample stacking [17,18], isotachophoresis [19,20], and solid-phase extraction [21], have been reported to increase the amount of sample injected and analyzed.

Due to the use of entire channel as the injection volume, the sample loading capacity of isoelectric focusing (IEF) is inherently greater than most chip-based electrokinetic separation techniques. Furthermore, IEF not only contributes to a high resolution protein/peptide separation based on their differences in isoelectric point (pI), but also potentially allows the analysis of low abundance proteins with a typical concentration factor of 50-100 times. To perform IEF, the entire channel is initially filled with a solution mixture containing proteins/peptides and carrier ampholytes for the creation of a pH gradient. Several research groups have recently reported the use of glass, quartz, or plastic-based microfluidics for demonstrating on-chip IEF separations [4,22-27].

Size Separation Using SDS Gel Electrophoresis

The current standard method for protein sizing, SDS-polyacrylamide gel electrophoresis (PAGE), is a labor-intensive technique. In comparison to SDS-PAGE, the significant advantages of performing SDS-protein separations in a capillary electrophoresis or microfluidic format [28-30] include: (i) the ability to use higher

electric fields resulting in rapid and ultrahigh resolution separations, (ii) improved reproducibility resulting from the use of replaceable polymeric sieving solution, and (iii) automated operation.

It has been reported that the formation of SDS-protein complexes is the critical step in determining separation resolution of capillary gel electrophoresis [31]. Once the SDS-protein complexes are properly formed, they remain relatively stable and the presence of SDS in the separation buffer is no longer needed for further stabilization. This is particularly true for rapid protein separation in capillary gel electrophoresis and microfluidics-based devices.

For laser-induced fluorescence detection of resolved proteins, however, SDS concentration has a significant effect on non-covalent protein labeling using the popular SYPRO dyes, which offer the benefit of low variations in fluorescent intensity between different proteins. The SYPRO probes, such as SYPRO orange and SYPRO red, are non-fluorescent in water but highly fluorescent in detergent, in which they take advantage of SDS binding to proteins to build a fluorescence-promoting environment. When the SDS concentration is above its critical micellar concentration (CMC), 8.3 mM (~0.24% in water and somewhat less in buffer solutions), the major portion of the staining dye in the electrophoresis buffer becomes attached to the SDS micelles instead of the SDS-protein complexes. In order to sensitively detect the resolved SDS-protein complexes, an on-chip SDS dilution step was incorporated between the separation channel and fluorescence detection [30]. The dilution step reduced the SDS concentration in the electrophoresis buffer from 0.25% (above CMC) to ~ 0.025% (below CMC). Such dilution disrupted the

SDS micelles, thereby allowing more dye molecules to bind to the SDS-protein complexes, prior to the detection.

Multidimensional Separation Techniques

The vast number of proteins present in the proteome of a typical organism requires that separations be performed on the mixture prior to introduction into the mass spectrometer for identification. For example, proteolytic cleavage of all yeast proteins with trypsin presents a highly complex peptide mixture of at least 300,000 peptides. The large variation of protein relative abundances having potential biological significance in mammalian systems (> 6 orders of magnitude) also presents a major analytical challenge for proteomics. Thus, total peak capacity improvements in multidimensional separation platforms are critically needed to enhance the dynamic range and detection sensitivity of mass spectrometry.

Assuming the separation techniques used in the two dimensions are orthogonal, i.e., the two separation techniques are based on different physicochemical properties of analytes, the peak capacity of two-dimensional (2-D) separations is the product of the peak capacities of individual one-dimensional methods [32]. Several systems have been reported which combine two individual orthogonal separations in coupled microchannels. Rocklin and co-workers have demonstrated 2-D separation of peptide mixtures in a microfluidic device using micellar electrokinetic chromatography and zone electrophoresis as the first and second dimensions, respectively [33]. Gottschlich et al. have also fabricated a spiral shaped glass channel coated with a C-18 stationary phase for performing reversed-phase chromatographic separation of trypsin-digested peptides [34].

By employing a cross interface, the eluted peptides from the micellar electrokinetic chromatography [33] or reversed-phase chromatography channel [34] were sampled by a rapid zone electrophoresis separation in a short glass microchannel. Additionally, Herr and co-workers have coupled IEF with zone electrophoresis for 2-D separations of model proteins using plastic microfluidics [27].

In each of these examples, the multiple separation dimensions are performed serially, without the ability to simultaneously sample all proteins or peptides separated in the first dimension for parallel analysis in the second dimension. As a step toward this goal, a microfabricated quartz device has been proposed by Becker and co-workers with a single channel for the first dimension and an array of 500 parallel channels with submicron dimensions as the second dimension positioned orthogonally to the first dimension channel [35]. However, the conceptual system is difficult to implement as described by Becker et al., and since its introduction in 1998 no published use of this device in performing 2-D bioseparations has been demonstrated. In a further step, Chen et al. recently described a 2-D capillary electrophoresis system based on a 6-layer PDMS microfluidic platform [26]. The system consisted of a 25 mm-long microchannel for performing IEF, with an intersecting array of parallel 60 mm-long microchannels for achieving SDS-PAGE. The system combines six individual layers of flexible PDMS, requiring the alignment, bonding, removal, re-alignment, and re-bonding of various combinations of the six layers to perform a full 2-D protein separation. This innovative system is somewhat cumbersome to implement, subject to band broadening due to diffusion during the post-separation assembly process, fairly complex due to the need for a reconfigurable three-dimensional microfluidic arrangement, potentially subject to cross-

contamination and potential arises for imperfect sealing of the various layers containing solutions of protein sample, buffers, and SDS during these manual manipulations. Nevertheless, instead of continuously sampling protein analytes eluted from the first separation dimension as in previously reported systems [27,33,34], this PDMS implementation represents a successful demonstration of parallel 2-D separations of multiple proteins (carbonic anhydrase, bovine serum albumin, and ovalbumin) in a microfluidic format.

1.3 PROJECT DESCRIPTION

This project aims to develop and validate a miniaturized and integrated 2-D protein separation platform based on non-native IEF and SDS gel electrophoresis in a single plastic microfluidic network. The ability to introduce and isolate two different separation media is one of two key requirements for performing the proposed 2-D protein separations. The second requirement lies in the quantitative transfer of protein analytes from the first to the second separation dimensions without significant loss in the resolution acquired from the first dimension. Instead of sequentially sampling protein analytes eluted from the first separation dimension, all focused proteins are simultaneously transferred and further resolved by SDS gel electrophoresis in a parallel and high throughput format. The ultrahigh sensitivity and extremely large dynamic range of fluorescence microscope detection is employed for the detection of resolved SDS-protein complexes in the microchannel array using non-covalent, environment-sensitive, fluorescent probes. The resulting instrumentation system only requires the use of minute protein samples and provides much greater automation, throughput, and sensitivity than existing 2-D PAGE technology.

Chapter two describes the development of a miniaturized membrane chromatography inside a commonly used capillary fitting for performing reversed-phase peptide separations. The miniaturized membrane chromatography system is further coupled with a micro(μ)-enzyme reactor containing immobilized trypsins for performing rapid protein digestion, peptide separation, and protein identification using electrospray ionization mass spectrometry. The use of miniaturized membrane chromatography allows

significant reduction in sample consumption together with enhanced detection sensitivity in comparison with those reported using μ-LC and capillary LC.

To further reduce the dead volume and sample consumption, Chapter three illustrates the use of plastic microfluidics for performing miniaturized IEF protein separations. A dynamic approach, which is based on electrokinetic injection of proteins/peptides from solution reservoirs, is demonstrated in this work to significantly increase sample loading and therefore the concentrations of focused proteins in microfluidics-based IEF separations. Dynamic sample introduction and analyte focusing in plastic microfluidic devices can be directly controlled by various electrokinetic conditions, including the injection time and the applied electric field strength. Differences in the sample loading are contributed by electrokinetic injection bias and are affected by the individual analyte's electrophoretic mobility. Under the influence of dynamic introduction and focusing, the protein sample loading is enhanced by approximately 10-100 fold in comparison with conventional IEF separations.

Additionally, a comprehensive polymer microfluidic network, combining non-native IEF with SDS gel electrophoresis, is reported in Chapter four. Rather than sequentially sampling protein analytes eluted from IEF, focused proteins are electrokinetically transferred into an array of orthogonal microchannels and further resolved by SDS gel electrophoresis in a parallel and high throughput format. Resolved protein analytes are monitored using non-covalent, environment-sensitive, fluorescent probes such as SYPRO Red. A 2-D protein separation is completed in less than 10 min with an overall peak capacity of around 1,700 using a chip with planar dimensions of as small as 2 cm x 3 cm. The novel aspects of this work include the development of a

multidimensional protein separation system that is capable of performing ultrahigh resolution analysis of complex protein mixtures such as cell lysates in a high throughput format using a single plastic microfluidic network. Implementing a conventional 2-D PAGE in a miniaturized platform enables proteome analyses to be performed at speeds unparalleled by competitive approaches.

CHAPTER 2

FUNDAMENTAL THEORIES

2.1 AMINO ACID AND PROTEINS

Proteins are the most abundant and essential biological molecules found in living cells. They serve a variety of vital functions such as controlling complex biochemical reactions and information pathways. Indeed, the word “protein” is actually derived from the Greek word “*proteios*”, meaning “first” or “principal”. All proteins, whether present in the most rudimentary bacteria or in more complex forms of life such as human beings, are composed of a common set of approximately 20 amino acids linked to each other in a large number. Despite the large variation in chemical and structural properties among different proteins, they are all derived from the same set of amino acids. The differentiation observed among different proteins is due largely to the number and sequence of amino acids included in the peptide chain.

The 20 standard amino acids observed in most naturally occurring proteins share common structural features (See Figure 2-1) [36]. These molecules are composed of carbon, hydrogen, oxygen, nitrogen, and sulfur in case of cysteine. They are all referred to as alpha(α)-amino acids since the amino group is bonded to the carbon atom adjacent to the carboxyl group. The additional carbons in the amino acid molecules are designated as β, γ, δ, and so forth. The α carbon is bonded to four different groups: a carboxyl group, an amino group, a hydrogen atom, and an R group, where R is the generic reference for the side chain of the amino acid. The properties of amino acids are mostly dependent on the side chains, which differ in structure, size, polarity and electric charge in water.

With the exception of glycine, the α carbon of all amino acids is a chiral center due to the four different groups bonded to it [37]. The presence of an asymmetric α carbon allows one chemical formula to provide two different structures. Such structures represent a class of stereoisomers called enantiomers. All amino acids found in naturally occurring proteins are present in the L-configuration. The configurations of amino acids are usually specified by the D, L naming system, which is based on the absolute configuration of the corresponding glyceraldehydes. Thus, the use of L and D system only refers to the relative configuration comparing with corresponding glyceraldehydes, and does not provide any information regarding the direction in optical activity. However, the relative configuration is important in a biochemical reaction because most of the active sites of enzymes are asymmetric and only L-amino acids have the proper orientation for enzymes to initiate the selected biochemical reaction.

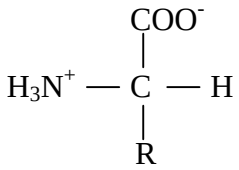

Figure 2-1 Common structure of an amino acid in Fischer projection formula

The 20 standard amino acids can be grouped into 5 classes which are based on the chemical properties of the side chains [36,38,40]. The polarity or tendency to interact with water at biological pH range is emphasized because it determines possible role an amino acid can play in peptides and proteins. The classifications of the 20 standard amino acids are shown in Figure 2-2 and some chemical properties of amino acids, including size, pI, and pKa of side chain, are summarized in Table 2-1.

Nonpolar groups

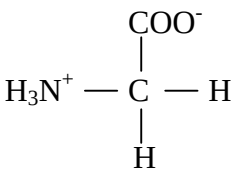

Glycine

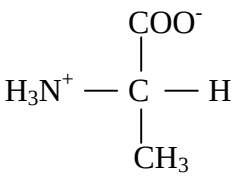

Alanine

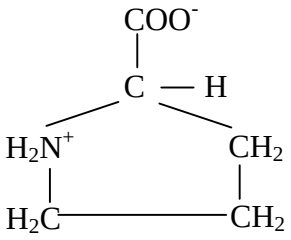

Proline

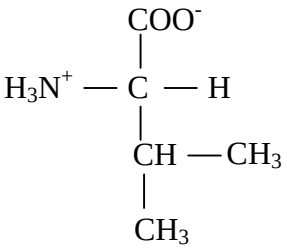

Valine

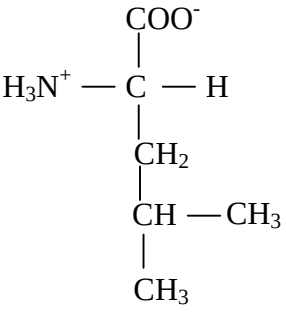

Leucine

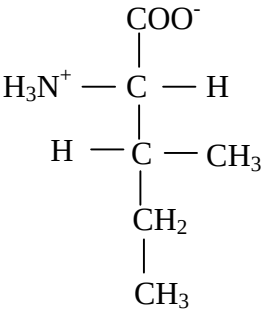

Isoleucine

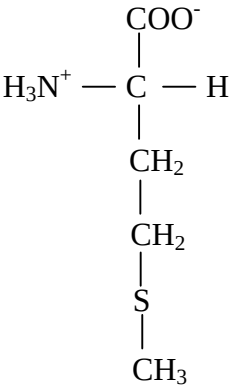

Methionine

Polar groups

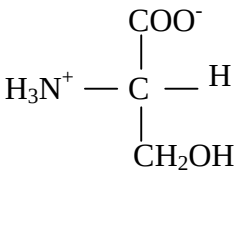

Serine

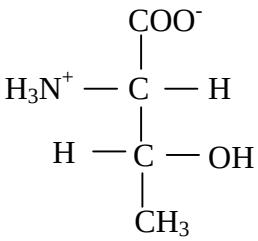

Threonine

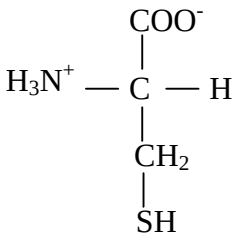

Cysteine

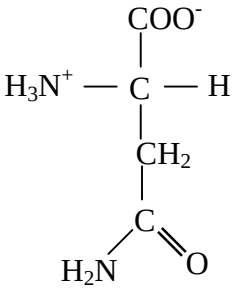

Asparagine

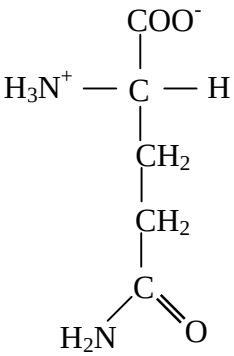

Glutamine

Positively charged groups

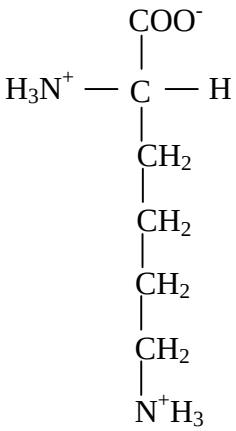

Lysine

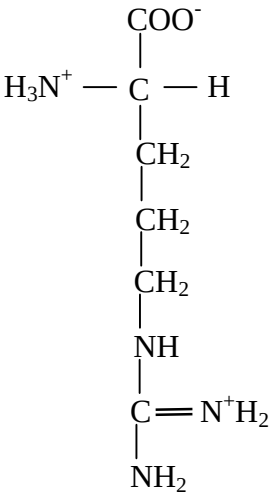

Arginine

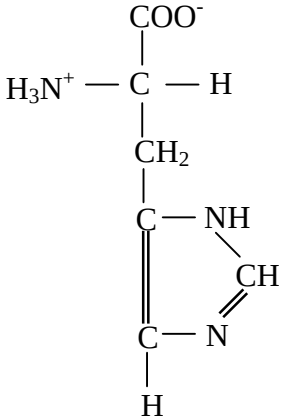

Histidine

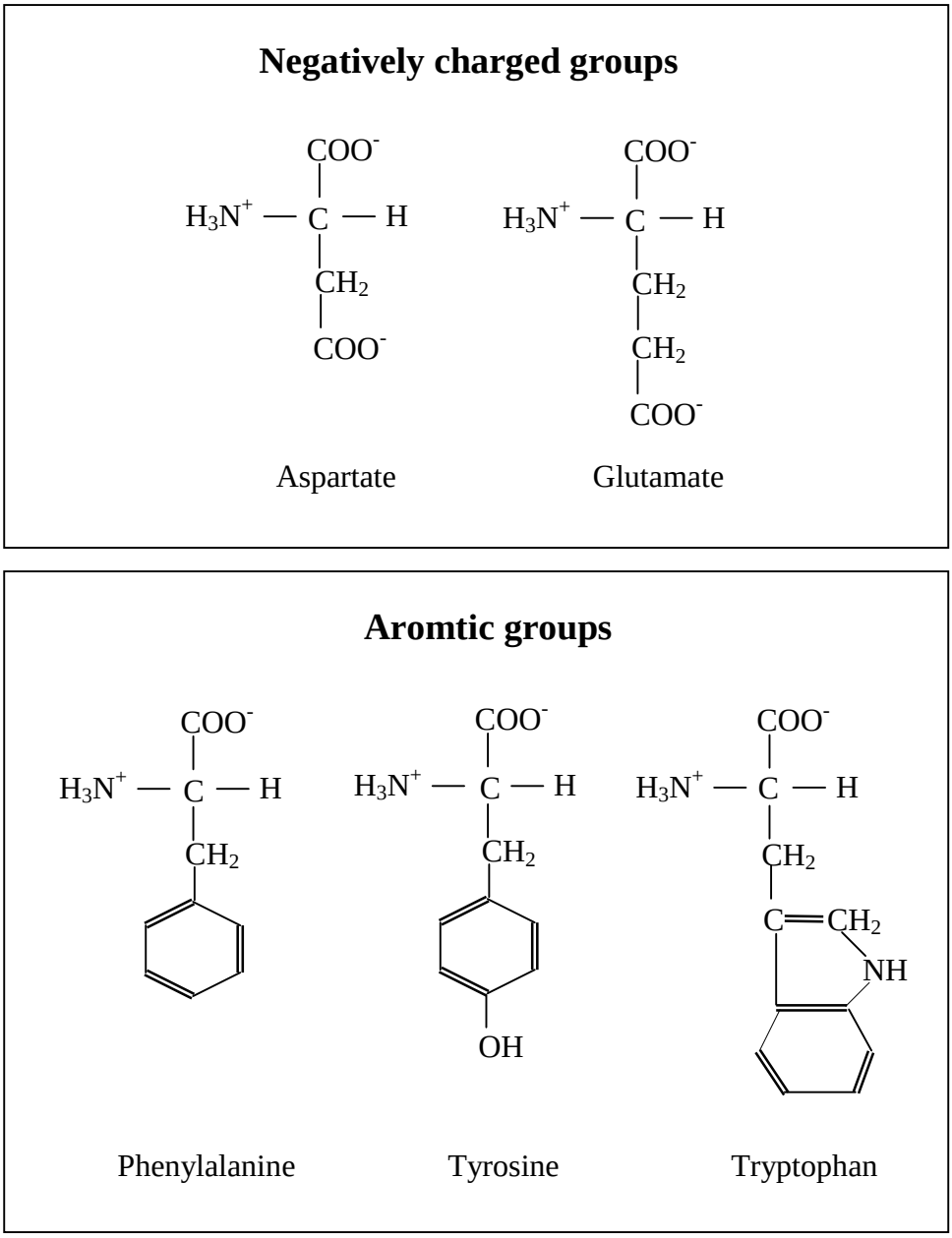

Figure 2-2 Structures of the 20 standard amino acids

Table 2-1 Properties and Conventions Associated with the Standard Amino Acids

Properties and Conventions Associated with the Standard Amino Acids									
Amino acid	Abbreviated names		M_r	pK_a values			pI	Hydropathy index	Occurrence in proteins (%)
				pK_1 (COOH)	pK_2 (NH_3^+)	pK_R (R Group)			
Nonpolar, aliphatic R groups									
Glycine	Gly	G	75	2.34	9.60		5.97	-0.4	7.2
Alanine	Ala	A	89	2.34	9.69		6.01	1.8	7.8
Proline	Pro	P	115	1.99	10.96		6.48	1.6	5.2
Valine	Val	V	117	2.32	9.62		5.97	4.2	6.6
Leucine	Leu	L	131	2.36	9.60		5.98	3.8	9.1
Isoleucine	Ile	I	131	2.36	9.68		6.02	4.5	5.3
Methionine	Met	M	149	2.28	9.21		5.74	1.9	2.3
Aromatic R groups									
Phenylalanine	Phe	F	165	1.83	9.13		5.48	2.8	3.9
Tyrosine	Tyr	Y	181	2.20	9.11	10.07	5.66	-1.3	3.2
Tryptophan	Trp	W	204	2.38	9.39		5.89	-0.9	1.4
Polar, uncharged R groups									
Serine	Ser	S	105	2.21	9.15		5.68	-0.8	6.8
Threonine	Thr	T	119	2.11	9.62		5.87	-0.7	5.9
Cysteine	Cys	C	121	1.96	10.28	8.18	5.07	2.5	1.9
Asparagine	Asn	N	132	2.02	8.80		5.41	-3.5	4.3
Glutamine	Gln	Q	146	2.17	9.13		5.65	-3.5	4.2
Positively charged R groups									
Lysine	Lys	K	146	2.18	8.95	10.53	9.74	-3.9	5.9
Histidine	His	H	155	1.82	9.17	6.00	7.59	-3.2	2.3
Arginine	Arg	R	174	2.17	9.04	12.48	10.76	-4.5	5.1
Negatively charged R groups									
Aspartate	Asp	D	133	1.88	9.60	3.65	2.77	-3.5	5.3
Glutamate	Glu	E	147	2.19	9.67	4.25	3.22	-3.5	6.3

Nonpolar or Hydrophobic Group

This group includes 7 amino acids and most of them, such as alanine, valine, leucine, isoleucine, and methionine, have nonpolar side chains. These amino acids can cluster together within the protein structure through weak hydrophobic interactions. Due to the large number of nonpolar amino acids found in proteins, the weak hydrophobic interaction provides the main source for stabilizing the protein's three-dimensional conformation. Glycine is the only standard amino acid without optical activity since it

lacks the chiral carbon. The secondary amino group in a cyclic structure of proline reduces the structural flexibility of polypeptides and proteins containing prolines.

Aromatic Group

This group is relatively nonpolar and contains various aromatic side chains. All three of these amino acids, phenylalanine, tyrosine, and tryptophan, can absorb light in the ultraviolet range since they contain conjugated aromatic rings. The three amino acids can participate in hydrophobic interactions with other amino acid residues. Additionally, tyrosine can form hydrogen bonds since it has hydroxyl group.

Polar or Hydrophilic Group

The side chains of these amino acids are hydrophilic or more soluble in water. Most of them can participate in hydrogen bond formation. This class of amino acids includes serine, threonine, cysteine, asparagines, and glutamine. The polarities of these amino acids are contributed by their hydroxyl groups (serine, threonine), sulfhydryl group (cysteine), and amide groups (asparagines, glutamine). Cysteine plays a special role in a protein's conformation. Two cysteine residues can be oxidized to form a covalently linked bond, which is called a disulfide bond (See Figure 2-3). The disulfide bonds provide covalent links within different parts of protein to form complex protein structures.

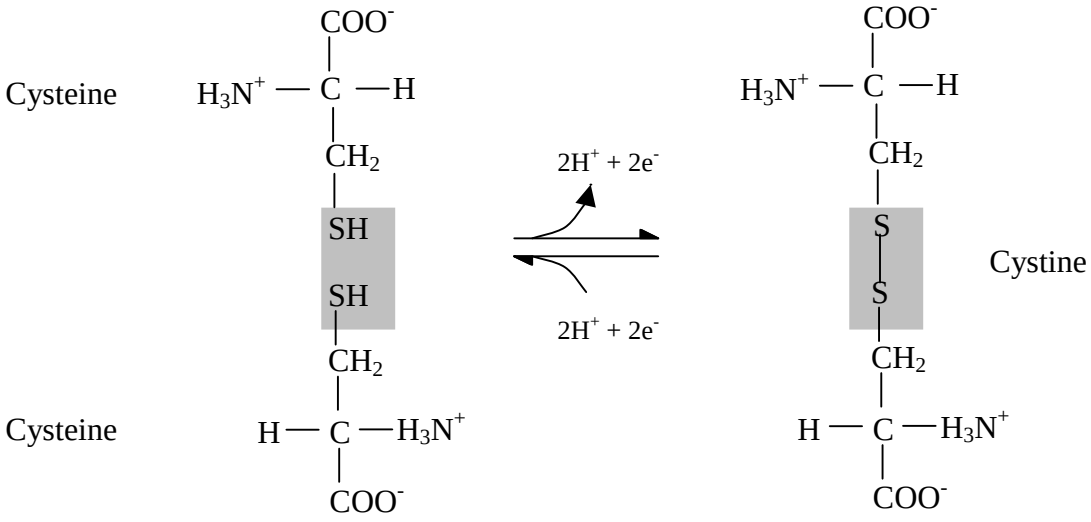

Figure 2-3 Formation of a disulfide bond by two molecules of cysteine

Positively Charged or Basic Group at pH 7

This group contains three amino acids of lysine, arginine, and histidine. These amino acids have more than half of their molecules present in a positively charged state at solution pH below the pKa of their side chains. They are more hydrophilic than polar group amino acids since they are positively charged in any biological environment close to neutral pH. Arginine contains a very basic guanidinium group, which is positively charged at most solution pHs. In contrast, histidine has a weakly basic imidazole group and is the only standard amino acid to have a side chain with a pKa near 7.

Negatively Charged or Acidic Group at pH 7

The side chains of aspartate and glutamate contain a second carboxyl group and have a net negative charge at pH 7. Asparagine and glutamine are the amide forms of aspartate and glutamate.

One important property of amino acids is that they can act as acids and bases in water. The dipolar ion (zwitterion) can lose a proton as an acid or proton donor:

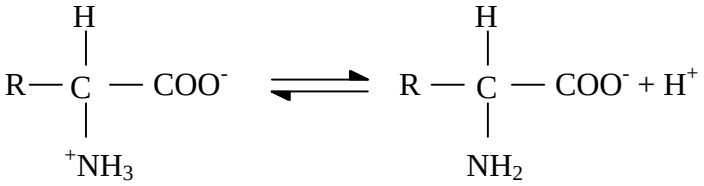

Zwitterion

or obtain a proton from solution as a base or proton acceptor:

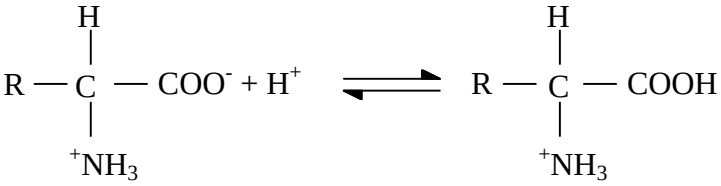

Zwitterion

The ionization of a standard amino acid is represented in the following equation with different charge states:

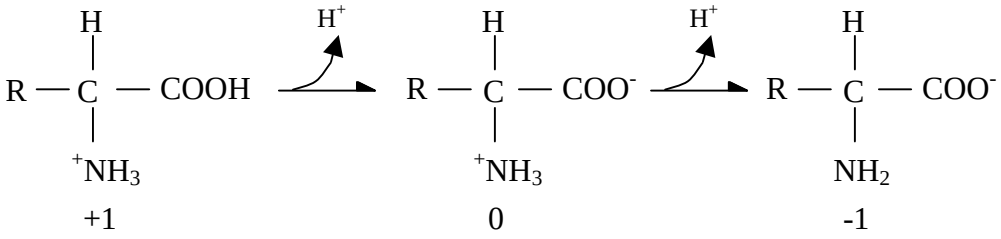

+1 0 -1

It is significant to note that the middle formula on the equation has a zero net charge, as the carboxyl group is ionized while the amino group is protonated. The formula of amino acids having one positive charge on the amino group and one negative charge on the carboxyl group is called zwitterion. The characteristic pH, at which the amino acid has no net charge and does not migrate under the influence of electric field, is called the isoelectric point (pI) of amino acid.

To study the acid-base properties and the pI values of amino acids, a titration curve is generated by adding or removing protons in amino acids. Glycine has no ionizable side chain as the simplest example [39]. The pI of glycine can be calculated simply by determining the arithmetic mean of the pK_1 (pK_a) and pK_2 (pK_b) values of the carboxyl and amino groups:

$$pI = \frac{1}{2}(pK_a + pK_b) = \frac{1}{2}(2.34 + 9.60) = 5.97$$

Those amino acids with ionizable side chains have more complex titration curves. For example, the histidine has an imidazole group as its side chain with a pK_R (pK_a) of 6.0 [36]. This imidazole group can be deprotonated with a pH higher than its pK_R, while the positive charge from the amino group can be neutralized by the negative charge of the carboxyl group. As a result, the net zero charge state of histidine occurs at solution pH between pK_R and pK_2 (see Figure 2-4). Thus, the pI of histidine, 7.59, is the average of pK_R (6.0) and pK_2 (9.17).

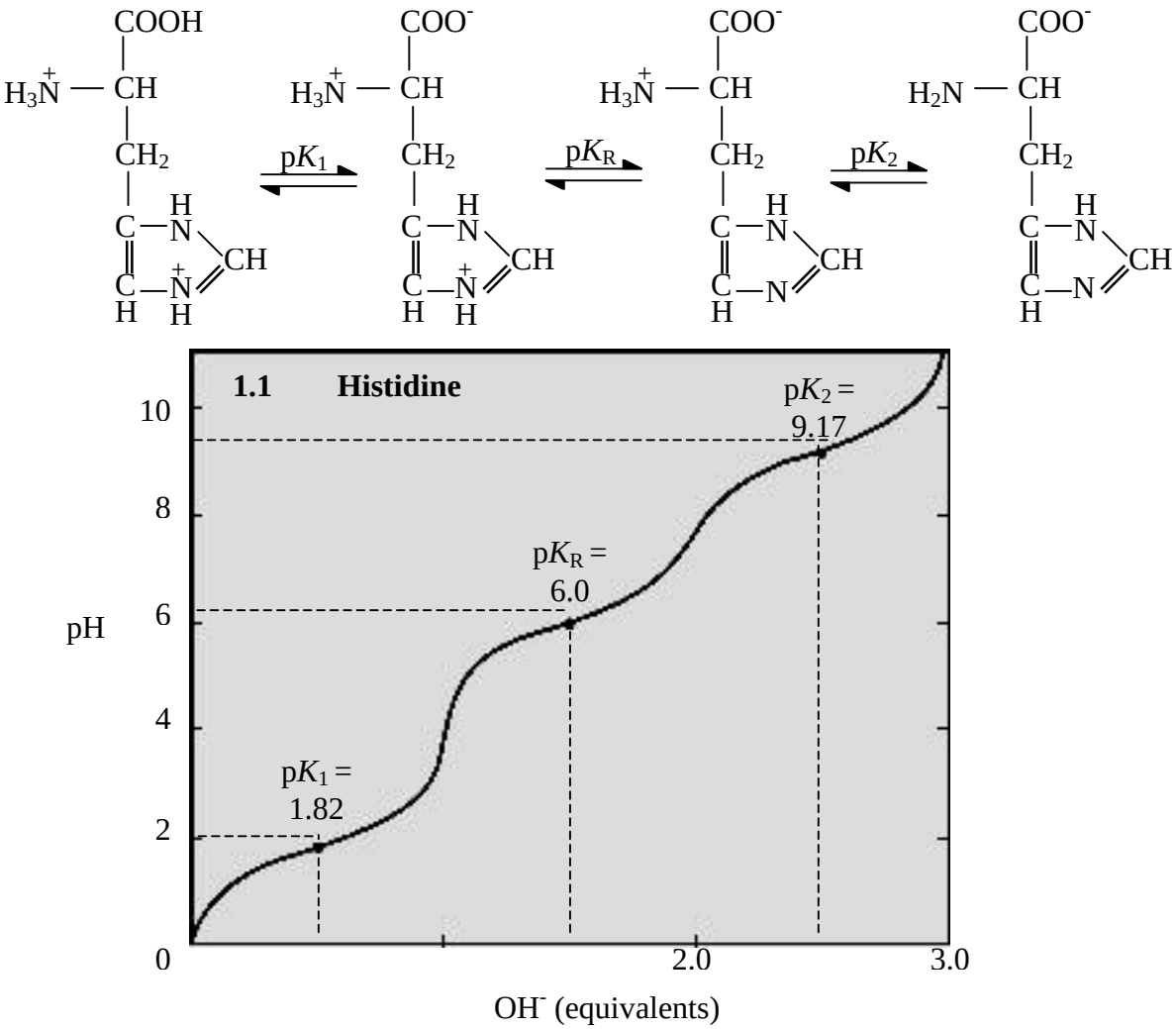

Figure 2-4 Titration curve of histidine

Since the amino acids are zwitterions in water and have flat stages in their titration curves, they are able to maintain solution pH in certain ranges. By forming a salt of acid or base, amino acids have the ability to minimize the effects of the added acid or base on the pH of the solution. In a physiological system, some amino acids, such as histidine, can be an effective buffer to provide an optimized environment for biological reactions.

A peptide consists of at least 2 amino acids. The amino acid residue at the end with a free α-amino group is called the amino-terminus or N-terminus. The residue with a free α-carboxyl group at the opposite end is called the carboxyl-terminus or C-terminus. The peptide polymer can be formed by a condensation reaction. In this reaction, two amino acids are covalently joined by bonding the carboxyl group of R_1-$CHNH_2$-COOH to the amino group of R_2-$CHNH_2$-COOH. One molecule of water is removed from the carboxyl group of R_1-$CHNH_2$-COOH and the amino group of R_2-$CHNH_2$-COOH (See Figure 2-5). This amide linkage is termed as a peptide bond.

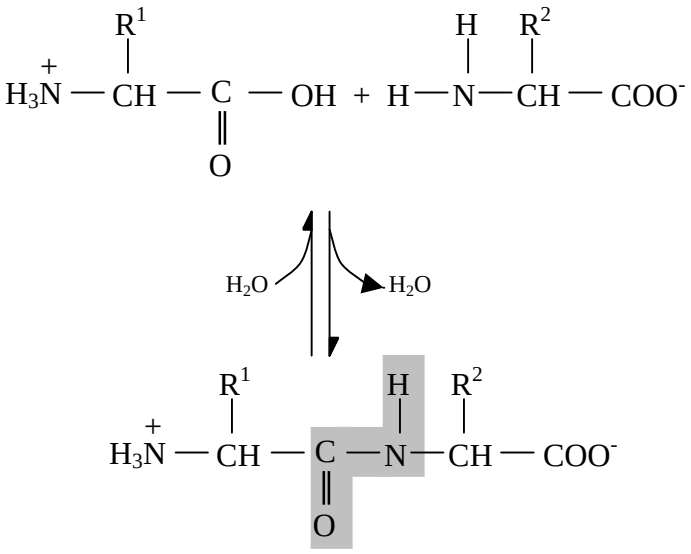

Figure 2-5 Formation of a peptide bond by condensation reaction

A protein is a large polymer consisting of thousands of amino acids. There is no precise line of definition between peptides and proteins. The exact sequences of amino acid residues in the protein are called protein primary structure. The unique properties of the individual protein are mainly based on the arrangement and the number of amino acids in its primary structure. After determination of the primary structure of a protein, a higher level of arrangement, which involves the presence of folding patterns of protein chain, is named as the secondary structure of protein. The most common secondary structures, including α-helix, β-sheet, and β-turn, are stabilized by hydrogen bonds among amino acids.

The tertiary structure and quaternary structure describe all detailed information in the three-dimensional structure. If the protein only contains one polypeptide chain, the arrangement of the folding structure is called the tertiary structure. It provides the protein size, shape, degree of extension, and helical conformation. Otherwise, the arrangement in space of a protein with multiple polypeptide subunits is represented as a quaternary structure. Figure 2-6 shows the different levels of structure in proteins. The hydrophobic interaction and dipole-dipole interaction are the two additional noncovalent forces that maintain protein's three-dimensional structure.

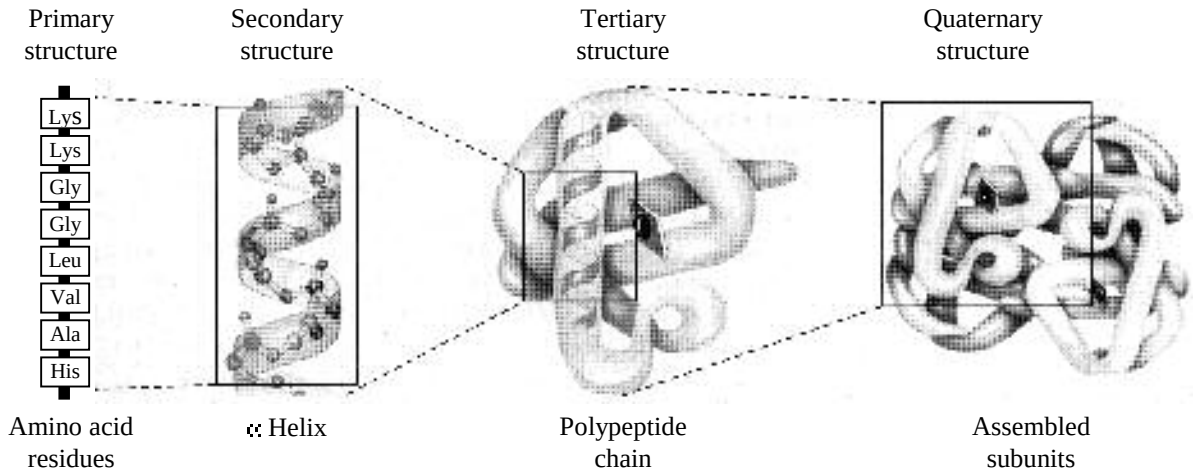

Figure 2-6 Different levels of structure in proteins

The net charge on a protein is given by:

$$\text{net charge} = \sum n_i/[(K_i/[\mathrm{H}^+]+1)] - \sum n_j/[([\mathrm{H}^+]/K_j+1)] \qquad (2\text{-}1)$$

where the molecule has *i* weakly basic groups and *j* weakly acidic groups. K_is and K_js are the ionization constants of basic and acidic moieties, respectively. The assumption is that the ionization constant of a specific moiety is unaffected by its position and neighboring amino acids. The solution pH, at which a protein has no net charge, is determined as the pI of that particular protein. Since a polypeptide or protein contains a large number of amino acid residues, the calculation of protein's pI is usually performed by computer software. Several Websites, including http://us.expasy.org, http://www.ncbi.nlm.nih.gov, and http://www.embl-heidelberg.de/cgi/pi-wrapper.pl, provide the on-line computation functions for the estimation of protein pI values.

2.2 ISOELECTRIC FOCUSING SEPARATIONS

Isoelectric focusing (IEF) is a member of a small family of equilibrium separation techniques, which includes density gradient centrifugation, equilibrium centrifugation, and gradient gel electrophoresis. Each of these techniques depends upon the establishment of a gradient in which analyte molecules are separated based on their differences in various molecular properties such as density (centrifugation), size (gradient gel electrophoresis), and isoelectric point (IEF). The main characteristic of these techniques is that the separation proceeds until equilibrium is reached, and no further resolution is achieved after this stage has been accomplished.

IEF has been applied almost exclusively to the resolution of polypeptides, because not all molecules possess an pI such as inorganic ions and oligonucleotides. Until recently, IEF has been primarily performed using gel as a matrix to eliminate convection and as a support for staining. It should be emphasized that the extremely high resolution of two-dimensional polyacrylamide gel electrophoresis (2-D PAGE) for protein separation is mostly contributed by IEF in the first separation dimension. By transferring IEF separation from gel to capillary format, the focusing effect of capillary isoelectric focusing not only contributes to a high resolution protein/peptide separation, but also provides a typical concentration factor of at least 100 times.

Capillary Isoelectric Focusing

The use of small diameter capillaries allows for the efficient dissipation of joule heat and permits the application of high voltages for rapid focusing of analyte proteins. The separations can therefore be performed in free solution without the need of gels. This allows the content of the capillary to be replaced between analyses and results in

improved reproducibility and analysis automation. The use of UV-transparent fused-silica capillaries enables direct on-line optical detection of a focused protein zone without the requirement of postseparation staining.

The pH gradient necessary to perform capillary isoelectric focusing is created by the carrier ampholytes. Ampholytes are mixtures of synthetic chemical species that posses slightly different pIs. For the creation of a pH gradient inside a capillary, the capillary is filled with a solution containing carrier ampholytes, which are constrained by an acidic solution (pH below the pI of most acidic ampholyte species) at the anode and an alkaline solution (pH above the pI of most basic ampholyte species) at the cathode.

Upon applying an electric field, all molecules with a net charge migrate towards the electrode of opposite charge. Because the ampholytes possess buffer capacity, they will maintain the pH at the location where they are focused. By employing a mixture of ampholytes with different pIs, a pH gradient begins to develop with low pH towards the anode and high pH towards the cathode. The range of the pH gradient in the capillary is defined by the composition of the ampholyte mixture.

In general, the combination of various ampholytes is employed for the formation of both narrow and wide pH gradients for performing IEF separations. For resolving proteins from cell lysates with broadly different pIs, a wide-range ampholyte blend is typically selected, e.g. the combination of ampholyte 3-5, 5-8, and 8-11. To prevent the basic proteins (pI equal to or greater than 10) from migrating into the catholyte by either diffusion or gradient shift, a basic compound such as N,N,N,N-tetramethylethylenediamine can be used to block the distal end of the channel [41]. Additionally, Mohan and Lee have demonstrated the use of N, N, N', N'-

tetramethylethylenediamine for extending the separation range to at least pI 12 [42]. In situations where enhanced resolution of proteins with similar pI values is desired, the use of narrow range ampholyte mixtures may be employed. Narrow range ampholyte mixtures generating gradients spanning 1 to 3 pH units are available from many commercial sources. Non-linear pH gradients can also be generated by adding a "separator" into the mixture of carrier ampholytes. The separator is an amphoteric molecule with a relatively high buffering power, which flattens the pH gradient near its pI [43].

During the performance of a capillary isoelectric focusing analysis, the capillary is filled with a solution containing amphoteric substance including carrier ampholytes and proteins. The focusing step begins with the immersion of the capillary in the anolyte (dilute phosphoric acid) and catholyte (dilute sodium hydroxide) solutions, followed by application of high voltage. While a pH gradient is established by carrier ampholytes, protein analytes at the same time migrate towards the electrode of opposite charge until a steady state is reached. At this point, each protein becomes focused in a narrow zone at its pI.

Focusing is achieved rapidly and is accompanied by an exponential drop in current. At the beginning of focusing, most components in the capillary such as carrier ampholytes and protein analytes have net charge and act as current carriers. When ampholytes and proteins reach their pIs, their net charge approaches zero and therefore the value of the current declines. Focusing is usually considered to be complete when the current has dropped to a level approximately 10% of its initial value and the rate of change approaches zero.

It is generally not advisable to prolong focusing because resistive heating increases the risk of protein precipitation. The solubility of concentrated proteins at their pIs, particularly for those highly hydrophobic species, may become a problem for the IEF separation. A whole family of non-detergent solubilizers, including glycols, sugars, and common zwitterions such as taurine, has been reported to greatly improve protein/peptide solubility in the proximity of their pIs [44, 46]. These additives can be employed for largely alleviating or completely preventing this solubility issue.

Because capillary electrophoresis instruments use on-column detection at a fixed point along the capillary, capillary isoelectric focusing must include a procedure of transporting the focused protein zones past the detection point. For hydrodynamic mobilization, focused protein bands are transported past the detection point by applying pressure or vacuum at one end of the capillary. Pressure can be created by compressed gas and height difference of liquid levels contained in the reservoirs. In general, voltage is applied during mobilization to maintain the protein zones focused.

For chemical mobilization, the chemical composition of the anolyte or catholyte is changed to cause a shift in the pH gradient, resulting in electrophoretic migration of focused protein zones past the detection point. At the completion of the focusing step, high voltage is turned off and the anolyte or catholyte is replaced by the mobilization reagent. The most common chemical mobilization method involves the addition of a neutral salt such as sodium chloride to the anolyte or catholyte.

By adding sodium chloride into the anolyte, sodium serves as the non-proton cation in anodic mobilization. Under the influence of applied potential, migration of the non-proton cation into the capillary results in a reduction in proton concentration, i.e., an

increase in pH. Progressive flow of non-proton cations therefore causes a progressive pH shift down the capillary, resulting in mobilization of proteins in sequence past the detection point near the anodic end. The pH shift occurs first near the anodic end of the capillary. Because small ions have a very high mobility, the pH transition is propagated quickly to the rest of the gradient.

Similarly, the presence of chloride ions in the catholyte functions as the non-hydroxyl anion in cathodic mobilization. By turning on the high voltage power supply, the migration of the non-hydroxyl anion into the capillary contributes to a reduction in hydroxyl concentration, i.e., a decrease in pH. Progressive flow of non-hydroxyl anions therefore causes a progressive pH shift down the capillary, resulting in mobilization of proteins in sequence past the detection point near the cathodic end. At the beginning of mobilization, current initially remains at the low value measured at the termination of focusing, but gradually begins to rise as the chloride ions enter the capillary. Later in mobilization, when chloride is present throughout the capillary, a rapid rise in current signals the completion of mobilization.

Isoelectric Focusing Theory and Its Implication to Chip-Based Separations

In IEF, the resolving power, $\Delta(pI)_{min}$, is controlled by

$$\Delta(pI)_{min} = 3\{(D/E)[(dpH/dx)/(-d\mu/dpH)]\}^{1/2} \quad (2\text{-}2)$$

where D is the diffusion coefficient of the species; E is the applied electric field strength; dpH/dx is the pH gradient; and dμ/dpH is the change of protein mobility against solution pH [41]. When substituting the definition of the applied electric field strength, E = V/L, in terms of applied potential, V, and the length of the separation channel, L, the resolving power is given by

$$\Delta(pI)_{min} = 3\{(D/V)[\Delta pH/(-d\mu/dpH)]\}^{1/2} \quad (2\text{-}3)$$

Thus, the minimum resolvable pI difference between adjacent focused bands is independent of channel length and dependent only upon the individual protein characteristics, the total pH difference across the separation channel, and the applied potential.

This capillary/channel length independence hypothesizes significant column miniaturization with minimal loss in the separation system performance. The limit to such miniaturization is determined by a maximum current density (joule heating) which, in turn, determines the maximum allowable voltage in the system. The degree of heat dissipation is directly controlled by the channel dimensions and materials. The miniaturization of the separation channel increases its surface area to volume ratio, allowing for the application of even higher electric field strengths than in conventional capillary electrophoresis. It should be noted that the thermal conductivity of the plastics being employed in this study for the fabrication of microfluidic devices are approximately 0.20 W/m-^{0}C and are at least five times smaller than that of fused-silica. Still, maximum achievable resolution can be obtained through voltage programming by ramping up the voltage during the focusing step, since the current decreases continuously as the result of protein focusing.

Due to the use of the entire channel as the injection volume, the sample loading capacity of IEF is inherently greater than most chip-based electrokinetic separation techniques. To perform IEF, the entire channel is initially filled with a solution mixture containing proteins/peptides and carrier ampholytes for the creation of a pH gradient. Several research groups have recently reported the use of glass, quartz, or plastic-based

microfluidics for demonstrating on-chip IEF separations [4, 22-27]. Instead of using carrier ampholytes, Macounova et al. have generated pH gradients as a result of the electrochemical decomposition of water for achieving protein separations in a microchannel [47,48].

However, the sample loading for on-chip IEF separations is still dependent on the initial analyte concentrations and microchannel dimensions, particularly the channel length. To significantly enhance sample loading and therefore the concentrations of focused analytes, dynamic introduction of proteins/peptides using electrokinetic injection from the solution reservoir has been demonstrated by Li and co-workers [49]. The proteins/peptides continuously migrate into the plastic microchannel and encounter a pH gradient established by carrier ampholytes originally present in the channel for focusing and separation. Dynamic sample introduction and analyte focusing are directly controlled by various electrokinetic conditions, including the injection time and the applied electric field strength. The sample loading is enhanced by approximately 10-100 fold in comparison with conventional IEF.

2.3 MICROFLUIDICS-BASED FIELD GRADIENT FOCUSING TECHNIQUES

In contrast to IEF, field gradient focusing methods [50,51] offer a broader field of application, particularly for protein/peptide separation and concentration. For example, proteins/peptides with extreme pI values may be outside the working pH range of IEF due to the limited availability of commercial ampholytes. Furthermore, the focused proteins/peptides in IEF are at their pIs where they have an increased tendency to

precipitate. To achieve field gradient focusing, proteins/peptides are focused by balancing the electrophoretic velocity of an analyte against the bulk velocity of the buffer containing the analyte. If there is an appropriate gradient in the electric field, the total velocity of the analyte as the sum of the bulk and electrophoretic velocities can be set to zero at a unique point along a channel. Instead of using a combination of electrodes and membranes for the generation of electric field gradient [51], Ross and Locascio have demonstrated the application of a temperature gradient together with an appropriate buffer for creating a corresponding gradient in the electrophoretic velocity of the analyte [52].

CHAPTER 3

MINIATURIZED MEMBRANE-BASED REVERSED-PHASE CHROMATOGRAPHY AND ENZYME REACTOR FOR PROTEIN DIGESTION, PEPTIDE SEPARATION, AND PROTEIN IDENTIFICATION USING ESI-MS

3.1 INTRODUCTION

Membrane chromatography has been introduced for solving two main issues encountered in scaling up chromatographic separations using fine particulate support media, namely technical challenges in overcoming high back pressure and slow solute diffusion kinetics [53]. Subsequently, fast chromatographic separations were achieved without applying extremely high pressure in membrane chromatography [54]. Since then, the applications of membrane chromatography have attracted great attention from pharmaceutical industries [55], particularly for protein separations [56]. Membrane chromatography has also been attempted to perform separations on non-protein target analytes such as DNA plasmids [57], oligonucleotides [58,59], peptides [58,60], amino acids [61,62], and small hydrophobic molecules [58].

In addition to membrane chromatographic separations, various proteins and enzymes have been immobilized on the compact and porous membrane media for performing affinity chromatography and enzyme reactions [63,64]. To miniaturize high performance membrane chromatography, two layers of polyvinylidene fluoride (PVDF) membrane, employed as the stationary phase, were sandwiched between two polydimethylsiloxane (PDMS) substrates containing microchannels [65]. On-line

coupling of miniaturized membrane chromatography with a miniaturized trypsin membrane reactor was demonstrated for protein digestion, peptide separation, and protein identification using electrospray ionization mass spectrometry (ESI-MS).

In addition to miniaturized reversed-phase membrane chromatography, two layers of PVDF membrane adsorbed with bovine serum albumin (BSA) were sandwiched between two PDMS substrates for performing chiral separation of racemic tryptophan and thiopental mixtures [66]. Based on the large surface area to volume ratio of porous membrane media, BSA adsorbed onto the PVDF membranes enables the high resolution separation of racemic mixtures with sample consumption of sub-nanogram or less in the integrated plastic microfluidics network. Furthermore, the utilization of membrane pore diameters in the submicron range effectively eliminates the constraints of diffusional mass-transfer resistance commonly encountered during chiral chromatography separations.

The void volume inside the two layers of PVDF membrane exposed to analyte molecules was estimated to be only 80 nl. However, most of the total dead volume in miniaturized membrane chromatography [65,66] was contributed by the capillary connections and microchannels. To significantly reduce the dead volume and the elution time, a commonly used capillary fitting is employed in this study for directly housing miniaturized membrane chromatography. By placing a hydrophobic and porous PVDF membrane around the end of a polymer sleeve, the assembly of capillary fitting, containing a length of fused-silica capillary, provides the necessary flow paths and the stationary phase for performing reversed-phase separations.

The capillary format of miniaturized membrane chromatography allows straightforward integration with UV absorbance detection and ESI-MS for analyte identification. On-line coupling of miniaturized membrane chromatography with a micro(μ)-trypsin membrane reactor through the use of a μ-sample injector is demonstrated for achieving rapid and effective protein digestion, peptide separation, and protein identification in an integrated and miniaturized platform. By comparing with the results obtained from μ-LC and capillary LC, the efficacy and the potentials of miniaturized membrane chromatography in tryptic mapping and protein identification are reported.

3.2 EXPERIMENTAL

Materials and Chemicals.

Bovine pancreatic trypsin and horse heart cytochrome C were purchased from Sigma (St. Louis, MO). Tris(hydroxymethyl)-aminomethane (Tris) and ultrapure urea were obtained from Bio-Rad (Hercules, CA) and ICN (Aurora, OH), respectively. Acetic acid, acetonitrile, methanol, and trifluoroacetic acid were acquired from Fisher (Fair Lawn, NJ). All solutions were prepared using water purified by a Nanopure II system (Branstead, Dubuque, IA) and further filtered with a 0.22 μm membrane (Millipore, Bedford, MA).

Construction of Miniaturized Membrane Chromatography Using Capillary Fitting

A miniaturized membrane chromatography system (see Fig. 3-1) was constructed using a capillary fitting (μ-tight true ZDV union) obtained from Upchurch Scientific (Oak Harbor, WA). The PVDF membranes with pore diameter of 0.1 μm (Immobilon-P^{SQ}) were acquired from Millipore (Bedford, MA). A small piece of PVDF membrane was curled widthwise and folded lengthwise over the end of a polymer sleeve containing a length of fused-silica capillary (50 μm i.d. and 192 μm o.d., Polymicro Technologies, Phoenix, AZ). It is important to note that the membrane overlapped the face of the sleeve in all directions, and the capillary was positioned flush to the end of the sleeve. The assembly of capillary, sleeve, and membrane was then slid inside the capillary fitting and properly tightened, providing the necessary seal for the membrane sandwiched between the sleeve and the capillary fitting housing.

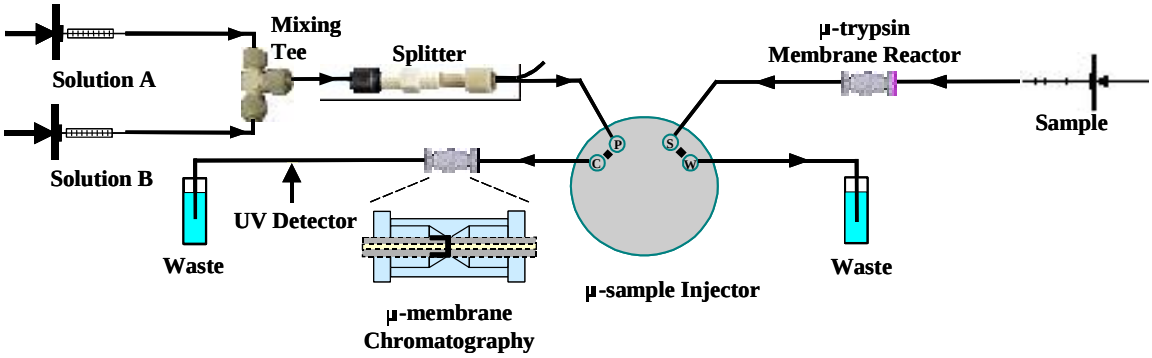

Figure 3-1 On-line coupling of μ-trypsin membrane reactor with miniaturized membrane chromatography through the use of a μ-sample injector. The inset presents the enlarged view of capillary fitting containing a piece of PVDF membrane

Assembly of μ-Trypsin Membrane Reactor

The components and procedures for assembly of a μ-trypsin membrane reactor inside a capillary fitting were the same as those utilized for the construction of miniaturized membrane chromatography. The immobilization of trypsin onto the PVDF membrane and detailed characterization of rapid and effective proteolytic digestion inside the reactor were reported in the previous work [67]. The ends of the capillary fitting were connected to a Harvard Apparatus 22 syringe pump (Holliston, MA) and the sample port of a 2-position/4-port μ-sample injector/switching valve (Valco Instruments, Houston, TX), respectively (see Figs. 3-1 and 3-2).

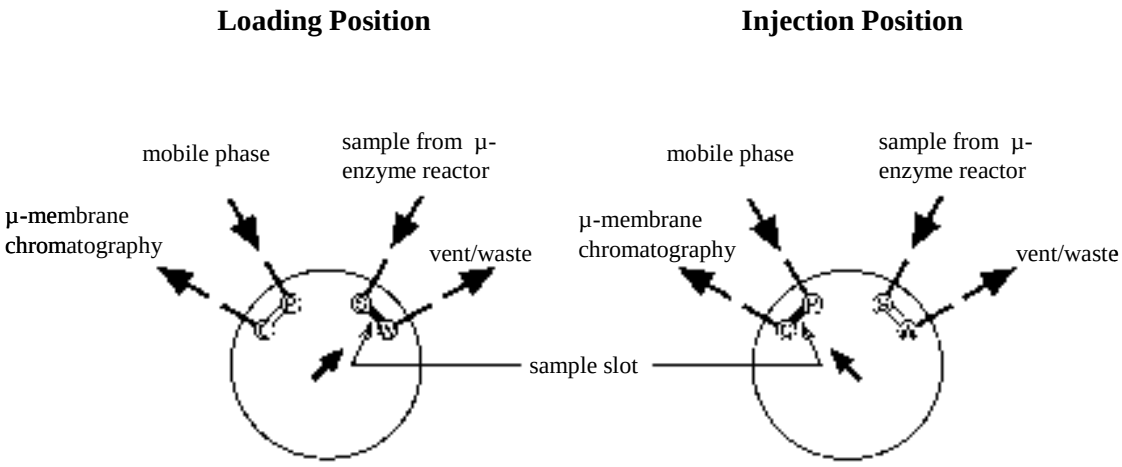

Figure 3-2 Schematic of loading and injection positions in a μ-sample injector. The injector contains four ports and can be switched between two positions for sample loading and injection.

Coupling of μ-Trypsin Membrane Reactor with Miniaturized Membrane Chromatography

Horse heart cytochrome C was completely denatured in a solution containing 8 M urea and 10 mM Tris overnight at room temperature. Denatured cytochrome C was reconstituted in a solution of 10 mM Tris and 1 M urea using Millipore microcentrifuge ultrafiltration filters (regenerated cellulose membrane, nominal molecular weight cutoff of 5,000). A 250 μl gas tight syringe (Hamilton, Reno, NV) was filled with a solution containing denatured and reconstituted cytochrome C at a concentration of 10 μg/ml. The protein solution was delivered into a μ-trypsin membrane reactor at a flow rate of 0.1 μl/min for performing trypsin digestion. The capillary exit in the reactor was connected to the sample port of a Valco μ-sample injector (see Fig. 3-1) for peptide sample loading and on-line coupling with miniaturized membrane chromatography.

The miniaturized membrane chromatography system was first flushed with a solution containing 20% acetonitrile (v/v) for 30 min and then equilibrated with deionized water for another 30 min at a flow rate of 0.1 μl/min. The cytochrome C digest from a μ-trypsin membrane reactor was introduced into a 0.1 μl injection loop inside a Valco μ-sample injector at a flow rate of 0.1 μl/min. By switching from the loading to the injection positions (see Fig. 3-2), the mobile phase delivered at a flow rate of 0.1 μl/min performed sample injection and peptide separation through the miniaturized membrane chromatography system.

Solvents A (0.1% trifluoroacetic acid in water) and B (0.1% trifluoroacetic acid in acetonitrile) were delivered by two separate Harvard Apparatus PHD 2000 programmable syringe pumps (see Fig. 3-1) for generating a linear gradient of 5-40% acetonitrile in 20

min. The mobile phase leaving a Upchurch μ-static mixing tee was carried at a flow rate of 10 μl/min. Prior to the mobile phase port of a Valco μ-sample injector, the flow rate was reduced to 0.1 μl/min using a Upchurch silica sealtight Y connector.

The other end of the capillary fitting housing miniaturized membrane chromatography was connected to a Linear 100 multi-wavelength detector (Linear Instruments, Reno, NV) or a sheath liquid interface prior to a Perkin-Elmer Sciex (Foster City, CA) API 150 EX single quadrupole mass spectrometer. The sheath liquid interface, which provided the necessary electrical connection for inducing the electrospray process, was constructed as described previously [68,69]. The sheath liquid, composed of 50% methanol, 49% water, and 1% acetic acid (v/v/v) at pH 2.6, was delivered by a Harvard Apparatus 22 syringe pump at a flow rate of 1 μl/min. An electrospray voltage of 4.0 kV was employed for generating a stable spray of resolved peptides eluted from miniaturized membrane chromatography. Peptides were measured by scanning from m/z 200 to m/z 1800 at a scan rate of 2 s/scan.

3.3 RESULTS AND DISCUSSION

High performance membrane chromatography has been successfully employed for the purification and separation of biological molecules [70-73]. In high performance membrane chromatography, layers of finely controlled and organized, microporous membrane are used as the stationary phase, and the functional ligands can be attached to the outer and inner surface areas of membrane. The membranes as the porous separation media can be in the forms of a compact and porous disk, a hollow fiber, and a rod. By comparing with HPLC, membrane chromatography exhibits the advantages of low

hydrodynamic pressure drop, rapid analysis, and less susceptibility to fouling and clogging. The use of various chromatography modes in membrane chromatography, including affinity, ion-exchange, hydrophobic interaction, and reversed-phase, is dependent on the chemical modification of membranes.

In this study, the miniaturized membrane chromatography was developed by securely placing a small piece of PVDF membrane at the tip of a polymer sleeve inside a commonly used capillary fitting. This PVDF membrane (Immobilon-P^{SQ}, pore diameter of 0.10 μm) is naturally hydrophobic and is designed for Western transfers and protein sequencing procedures. The porous structure of this PVDF membrane provides a large internal surface area (~400 cm^2/cm^2 of front surface) for peptide interaction. Thus, the capillary fitting containing fused-silica capillaries not only provides the stationary phase for performing reversed-phase peptide separations, but also affords all of the necessary flow connections with minimized dead volume.

Furthermore, the miniaturized membrane chromatography device was coupled to a μ-trypsin membrane reactor for achieving on-line protein digestion and peptide separation. As discussed in previous studies [67], the extent of protein digestion in a membrane-based enzyme reactor can be directly controlled by the residence time of protein analytes inside the trypsin-immobilized membrane, the reaction temperature, and the protein concentration. The residence time of protein analytes, in turn, is a function of membrane thickness, polymer sleeve dimensions (in the capillary fitting), and protein infusion rate. By applying the same experimental conditions as those reported previously [67], complete digestion of cytochrome C was anticipated with a residence time of only ~

30 s and the resulting cytochrome C peptides were directly introduced into miniaturized membrane chromatography using a μ-sample injector (see Fig. 3-1).

As shown in Fig. 3-3A, cytochrome C peptides were eluted by a linear mobile phase gradient of 5-40% in 20 min and were detected by UV absorbance at 214 nm. Approximately 70 femtomole of digested cytochrome C sample from the μ-trypsin membrane reactor was injected for the separation. Theoretically, there should be 21 peptides in the cytochrome C digest based on the specificity of trypsin and the sequence of cytochrome C. For several reasons, less than the theoretical number of peptides is frequently seen and reported for tryptic digests. One is that very small, hydrophilic peptides elute from a reversed-phase column unretained. Another is that similar peptides may co-elute during the separation.

By comparing with the separation results obtained from capillary LC and μ-LC (see Figs. 3-3B and 3-3C), the number of peaks in the three chromatograms is roughly the same. However, there are differences in the experimental conditions and detection sensitivities that should be noted. One difference was the use of a capillary window with the dimensions of 100 μm i.d. x 200 μm o.d. for UV detection in μ-LC and capillary LC. The capillary window employed for miniaturized membrane chromatography had the dimensions of 50 μm i.d. x 200 μm o.d. By taking into account the difference in optical path length for absorbance detection, the concentration of eluted cytochrome C peptides from miniaturized membrane chromatography (Fig. 3-3A) was comparable to that measured in μ-LC (Fig. 3-3C), and was about 30-50% of that obtained from capillary LC (Fig. 3-3B).

Figure 3-3 Comparison of cytochrome C peptide separations achieved by (A) miniaturized membrane chromatography: 70 femtomole sample loading, a linear gradient of 5-40% acetonitrile in 20 min at a flow rate of 0.1 μl/min, and UV detection at 214 nm; (B) capillary LC: 25 pmole sample loading, a linear gradient of 5-40% acetonitrile in 20 min at a flow rate of 2 μl/min, 150 μm i.d. x 10 cm reversed-phase C_{18} column, UV detection at 214 nm; (C) μ-LC: 150 pmole sample loading, a linear gradient of 10-40% acetonitrile in 15 min at a flow rate of 40 μl/min, 1 mm i.d. x 15 cm reversed-phase C_{18} column, UV detection at 214 nm.

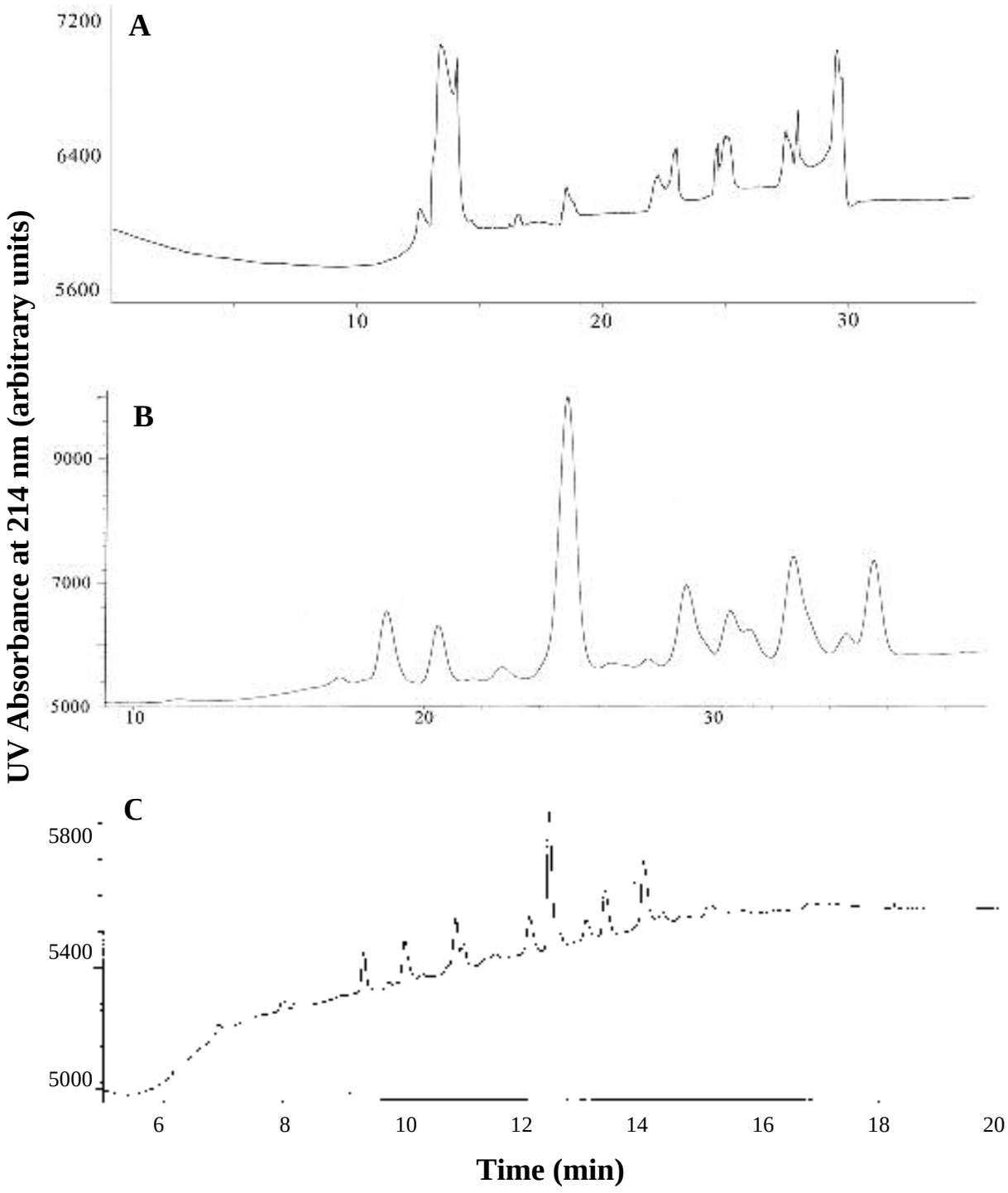
A
7200
6400
5600
10
20
30
B
9000
7000
5000
10
20
30
C
5800
5400
5000
6
8
10
12
14
16
18
20
UV Absorbance at 214 nm (arbitrary units)
Time (min)

However, approximately 150 pmole of cytochrome C peptides from overnight proteolytic digestion using solution trypsin was injected for the separation in μ-LC. The sample consumption for capillary LC was decreased to 25 pmole and was still at least three hundred times of that utilized in miniaturized membrane chromatography. The volume flow rate of organic solvent gradient was 40 μl/min for μ-LC and was reduced to 2 μl/min and 0.1 μl/min for capillary LC and miniaturized membrane chromatography, respectively. Furthermore, the separation efficiency measured from miniaturized membrane chromatography was lower than those obtained from μ-LC and capillary LC. The poor separation efficiency of miniaturized membrane chromatography was mainly contributed by potential channeling through the membrane media which was not optimized for performing the separation.

A miniaturized membrane chromatography system was reported and demonstrated in previous studies [65] by sandwiching two layers of PVDF membrane between two PDMS substrates containing microchannels. By comparing with previous results [65], an approximately 400-fold decrease of sample consumption was achieved by miniaturized membrane chromatography constructed in this study. Furthermore, the void volume was reduced by at least one order of magnitude. As the result, the elution times of cytochrome C peptides were significantly shortened and were comparable with those in μ-LC and capillary LC with considerably higher mobile phase flow rates (see Fig. 3-3).

Instead of using UV detection, the capillary format of miniaturized membrane chromatography makes it possible to directly couple with a sheath liquid interface for performing ESI-MS detection of eluted cytochrome C peptides. On-line ESI-MS analysis of separated cytochrome C peptides from miniaturized membrane chromatography is

shown in Fig. 3-4. By comparing with the results shown in Fig. 3-3A, the increase in the migration time of cytochrome C peptides was attributed to the increase in the dead volume associated with the sheath liquid interface and an additional capillary connection. The sheath liquid interface, which provided the necessary electrical connection for inducing the electrospray process, possibly contributed to additional band broadening as observed in the total ion current (TIC) chromatogram (see Fig. 3-4). All of the cytochrome C peptides in the TIC chromatogram were directly identified on the basis of mass spectra taken from the average scans under the peaks. The mass spectra of peptides taken from the average scans under the peaks with the elution times of 23.3 min, 25.8 min, and 27.3 min are shown in Fig. 3-5. The amino acid sequence of each peptide was obtained by searching the database using the mass as the constraint.

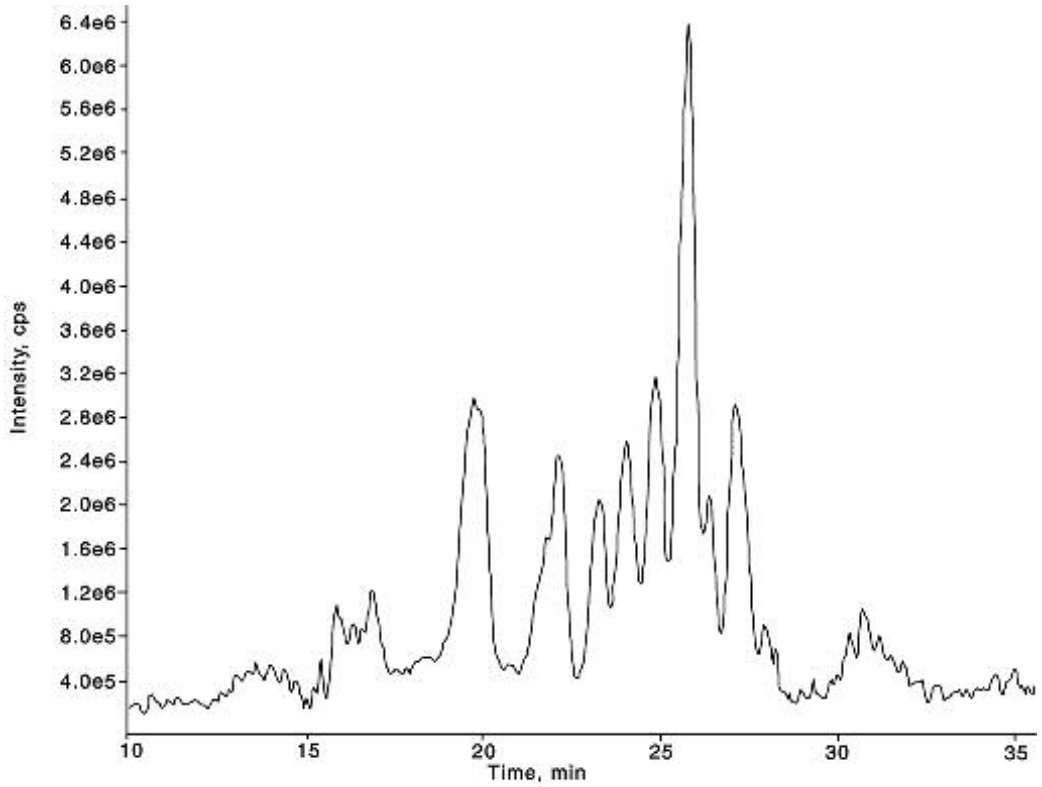

Figure 3-4 Total ion current monitoring of cytochrome C peptides eluted from miniaturized membrane chromatography using the positive ESI mode.

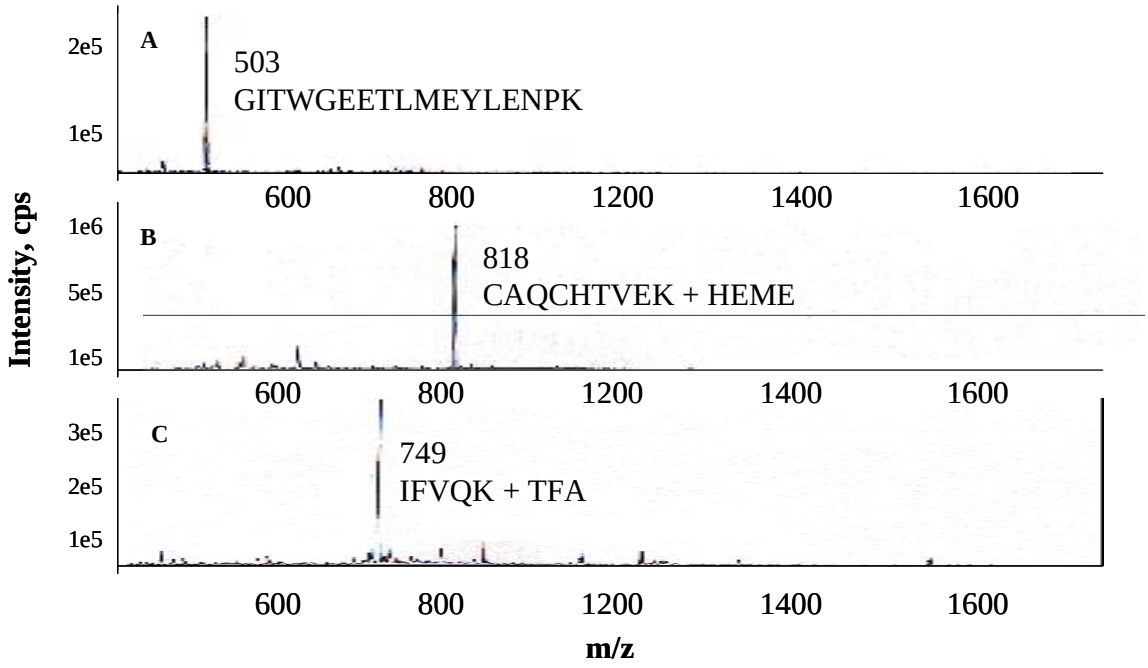

Figure 3-5 Positive ESI mass spectra taken from the average scans under the peaks with the elution times of (A) 23.3 min, (B) 25.8 min, and (C) 27.3 min in Fig. 3-4.

3.4 CONCLUSION

On-line coupling of a μ-trypsin membrane reactor with miniaturized membrane chromatography is developed and demonstrated as an integrated microanalytical tool enabling rapid protein digestion, high resolution peptide separation, and sensitive protein identification using ESI-MS. The combination of chromatographic separation with ESI-MS contributes to further enhancement in the dynamic range and the detection sensitivity for the analysis of a protein digest. Such enhancement is particularly attractive for the analysis of complex protein mixtures with a significant difference in their individual concentrations.

CHAPTER 4

DYNAMIC ANALYTE INTRODUCTION AND FOCUSING IN PLASTIC MICROFLUIDIC DEVICES FOR PROTEOMIC ANALYSIS

4.1 INTRODUCTION

The finalization of the sequencing of the human genome is opening the door for fundamental understanding of complex biological processes, including development, differentiation, and signal transduction. These processes typically involve the coordinated expression of multiple genes and proteins, as well as control of their function. However, the studies of oligonucleotide and protein mixtures of biological origin often impose significant analytical challenge due to their complexity and low abundance.

Recent trends to overcome cumbersome and expensive methodologies currently employed in laboratories involve the development of miniaturized and integrated total chemical analysis system. Over the last decade, the field of microfluidic devices has spread out for a variety of applications in genomic [74-80] and proteomic analyses [14,30,33,34,81-84]. The use of microfabricated devices clearly provides significant advantages over bench-top instruments, including smaller dead volume, smaller sample consumption, shorter analysis time, higher reproducibility, lower cost, and greater separation resolution in a multidimensional format [33,34].

Among various electrokinetic-based separation techniques, isoelectric focusing (IEF) not only contributes to a high resolution protein separation with a pI difference as small as 0.005 pH unit [43], but also potentially allows the analysis of low abundance

proteins with a typical concentration factor of 50-100 times. To perform IEF, the entire channel is initially filled with a solution mixture containing proteins/peptides and carrier ampholytes for the creation of a pH gradient. Several research groups have recently reported the use of glass or plastic-based microfluidics for demonstrating on-chip IEF separations [4,22,24-26,85]. Instead of using carrier ampholytes, Macounova et al. [47] have generated pH gradients as a result of the electrochemical decomposition of water for achieving protein separations in a microchannel.

Sample loading, particularly for the analysis of low abundant proteins in complex protein mixtures such as cell lysate, is a critical issue for capillary electrophoresis, and even more significant for on-chip electrophoretic separations due to limited microchannel dimensions. For example, the limited injection volume in zone electrophoresis usually renders the separation method unsuitable for proteomic applications. Thus, various concentration strategies, including sample stacking [17], isotachophoresis [19], and solid-phase extraction [21], have been reported to increase the amount of sample injected and analyzed.

Due to the use of entire channel as the injection volume, the sample loading capacity of IEF is inherently greater than most chip-based electrokinetic separation techniques. However, the sample loading for on-chip IEF separations is still dependent on the initial analyte concentrations and microchannel dimensions, particularly the channel length. To significantly enhance sample loading and therefore the concentrations of focused analytes, dynamic introduction of proteins/peptides using electrokinetic injection from the solution reservoir is demonstrated in this study.

The plastic microchannel employed for dynamic introduction is initially filled with only a carrier ampholyte solution. Upon the application of electric potentials, a pH gradient inside the channel is rapidly established, contributed by the presence of the small and highly mobile carrier ampholytes. Proteins/peptides continuously migrate into the channel and encounter the pH gradient for focusing and separation. As the result of electrokinetic-based injection and focusing, several factors, including injection time and analyte mobility, are investigated for controlling sample loading and focused analyte concentration.

4.2 MATERIALS AND METHODS

Materials and Reagents

An engineered green fluorescence protein variant (EGFP), which fluoresces (excitation: 488 nm; emission: 507 nm) 35 times more intensively than wild-type GFP, was obtained from Clontech (San Francisco, CA). BODIPY® FL bovine serum albumin (BSA) conjugate (excitation: 501 nm; emission: 509 nm) and the fluorescein conjugated peptide of formyl-Nle-Leu-Phe-Nle-Tyr-Lys (excitation: 497 nm; emission: 517 nm) were purchased from Molecular Probes (Eugene, OR). Pharmalyte 3-10 was acquired from Amersham Pharmacia Biotech (Uppsala, Sweden). Ammonium hydroxide, BSA, dithiothreitol, hydrofluoric acid, phosphoric acid, and potassium hydroxide were obtained from Sigma (St. Louis, MO). All aqueous solutions were prepared using water purified by a Nanopure system (Dubuque, IA) and filtered with 0.1 μm filter unit from Millipore Corporation (Bedford, MA).

Fabrication of Silicon Templates

The fabrication of a silicon template was performed by following standard procedures involving photolithography and chemical etching. Briefly, the 2.4 μm-thick silicon dioxide surface of the <100> oriented p-type silicon wafer (WaferNet, San Jose, CA) was covered by a layer of photoresist. Then, a patterned photomask, which consisted of the channel design printed with high resolution onto a transparency, was placed on top of the photoresist layer.

Following the exposure of the wafer to ultra-violet light, the photoresist was developed to form the desired patterns and features on the wafer surface. The wafer was then etched with buffered hydrofluoric acid solution to remove the silicon dioxide except for that under the protection of the developed photoresist. The remaining silicon dioxide pattern acted as a protection mask so that the silicon could be etched anisotropically in 45% (w/v) potassium hydroxide solution to form a positive relief mold containing the desired three-dimensional structures for the fabrication of plastic microchannels.

Fabrication of Plastic Microchannels

The PDMS base and curing agent from a Sylgard® 184 kit (Dow Corning, Midland, MI) were mixed 10:1 (v/v) and poured over the silicon template, which was fixed in a large petri dish. The template provided a positive relief mold for the formation of the channel in the PDMS substrate. The PDMS was allowed to cure at 60 ^{o}C for 1 hour in an oven. The 2 mm thick PDMS slab was carefully removed from the template after curing. The open channel on the PDMS substrate was sealed with another layer of PDMS film containing holes (0.5 cm in diameter) as solution reservoirs for fluid access.

Pieces of plastic substrates, 9.0 cm in diameter, were cut from the polycarbonate (PC) sheet (Sheffield Plastic, Sheffield, MA) for imprinting microchannels with a silicon template. The PC substrate was placed over the silicon template and the whole assembly was sandwiched between two glass plates. A hydraulic press was employed to apply a pressure of 900 psi at 160 ^{o}C for 5 min. After the pressure was released, the PC substrate containing imprinted microchannel was cooled down and subsequently removed from the press. The open microchannel was aligned with another PC substrate containing drilled holes for fluid access. To achieve thermal bonding between two PC substrates, the whole assembly was again sandwiched between two glass plates and placed inside the press under 300 psi and 138 ^{o}C for 10 min.

Isoelectric Focusing of Proteins/Peptides in Plastic Microchannels

To perform conventional IEF separations, a 1.2-cm-long microchannel (100 μm in width and 40 μm in depth) fabricated on the PDMS or PC substrate was filled with a solution containing protein analytes (2.5 ng/μL BSA conjugate and 1.0 ng/μL EGFP) and 2% pharmalyte 3-10. Focusing was performed at various electric field strengths using a CZE 1000R high-voltage power supply (Spellman High-Voltage Electronics, Plainview, NY). The solutions of 10 mM phosphoric acid (pH 2.8) and 0.5% ammonium hydroxide (pH 10.5) were employed as the anolyte and the catholyte, respectively. Protein focusing was monitored by a Nikon fluorescence microscope (Melville, NY) which was equipped with a high sensitivity charge-coupled device camera from Andor Technology (Belfast, Northern Ireland).

For dynamic introduction and focusing, the microchannel was filled with a solution containing only 2% pharmalyte 3-10. The fluorescein conjugated peptide of formyl-Nle-Leu-Phe-Nle-Tyr-Lys with a concentration of 1.0 ng/μL was prepared using the anolyte solution (10 mM phosphoric acid) containing 10 mM dithiothreitol and placed in the anodic reservoir. The presence of dithiothreitol prevented the peptide in the anodic reservoir from being oxidized during dynamic introduction and focusing. However, the green fluorescence of EGFP was irreversibly reduced at acidic pH as the result of protein denaturation. Thus, EGFP known to be stable up to pH 11 was prepared using the catholyte solution (0.5% ammonium hydroxide) with a final concentration of 1.0 ng/μL and placed in the cathodic reservoir. Dynamic enhancements in sample loading and analyte concentration were investigated using various injection times at constant electric field strength of 500 V/cm.

4.3 RESULTS AND DISCUSSION

In isoelectric focusing, the resolving power, $\Delta(pI)_{min}$, is controlled by

$$\Delta(pI)_{min} = 3\{(D/E)[(dpH/dx)/(-d\mu/dpH)]\}^{1/2} \quad (3\text{-}1)$$

where D is the diffusion coefficient of the species; E is the applied electric field strength; dpH/dx is the pH gradient; and dμ/dpH is the change of protein mobility against solution pH (86). When substituting the definition of the applied electric field strength, E = V/L, in terms of applied potential, V, and the length of the separation channel, L, the resolving power is given by

$$\Delta(pI)_{min} = 3\{(D/V)[\Delta pH/(-d\mu/dpH)]\}^{1/2} \quad (3\text{-}2)$$

Thus, the minimum resolvable pI difference between adjacent focused bands is independent of channel length and dependent only upon the individual protein characteristics, the total pH difference across the separation channel, and the applied potential. This channel length independence hypothesizes significant column miniaturization with minimal loss in the separation system performance. The limit to such miniaturization is determined by a maximum current density (joule heating) which, in turn, determines the maximum allowable voltage in the system.

Conventional Isoelectric Focusing Separations in Plastic Microfluidic Devices

In the presence of carrier ampholytes, adsorption of the ampholytes onto the plastic channel walls, including PDMS and PC employed in this study, eliminates the electroosmotic flow. This is evidenced by the lack of movement of focused protein bands after the focusing is complete. The lack of electroosmosis in IEF separations is further supported by the previous work using fused-silica capillaries [87]. Due to the use of only 1.2-cm-long microchannels for performing IEF separations, the images of focused analyte bands are directly monitored using a fluorescence microscope without the need for band mobilization.

PDMS is a material that has some unique features [88] making it useful for various microfluidic applications. The low background associated with PDMS implies that it may be a better substrate than many other plastic materials for fluorescence

detection. Furthermore, PDMS is chemically and physically inert, electrically insulating, and inexpensive. However, the adsorption of protein analytes onto the channel wall significantly reduces the separation efficiency and resolution obtained using the unmodified PDMS substrates (see Fig. 4-1A). Only one broad protein band containing EGFP and BSA conjugate is observed after focusing is complete.

The PDMS substrate can be oxidized in oxygen plasma. The plasma introduces silanol groups (Si-OH) at the expense of methyl groups ($Si-CH_3$) [7,8]. Thus, oxidation of the PDMS renders the surface hydrophilic due to the presence of silanol groups. Furthermore, the oxidized PDMS surface allows covalent attachment of trichlorosilanes and opens the possibility for the surface attachment of hydrophilic polymers such as polyacrylamide for reducing protein adsorption onto the channel wall [89,90].

Instead of performing covalent surface modifications, the use of PC substrate for IEF separations was investigated in this study. To further reduce protein adsorption, the plastic devices were initially flushed with a BSA solution (5 mg/mL in 10 mM Tris at pH 8) prior to the introduction of a solution mixture containing protein analytes and carrier ampholytes. The baseline bandwidths of BSA conjugate and EGFP measured from the PDMS and PC devices are summarized in Table 4-1. Clearly, the combined usages of PC substrate with BSA pretreatment provides significant improvement in separation efficiency and resolution.

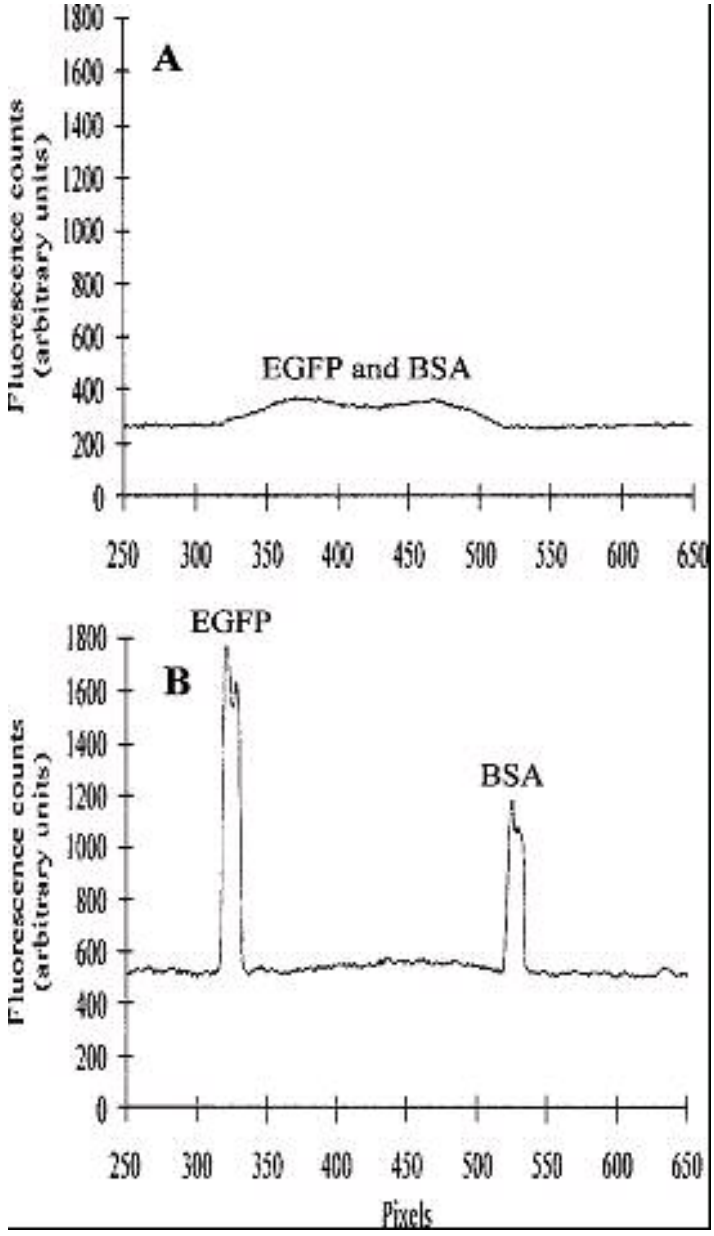

Figure 4-1 IEF separations of BSA conjugate and EGFP using (A) unmodified PDMS substrate and (B) PC substrate pretreated with BSA. Microchannel: 100 mm in width, 40 mm in depth, 1.2 cm in length; sample mixture: 2% pharmalyte 3-10, 2.5 ng/mL BSA conjugate, and 1.0 ng/mL EGFP; anolyte: 10 mM phosphoric acid (pH 2.8); catholyte: 0.5% ammonium hydroxide (pH 10.5); electric field strength: 500 V/cm.

Baseline resolution of BSA conjugate and EGFP (see Fig. 4-1B) was achieved using a 1.2-cm-long PC microchannel pretreated with BSA. The BSA peak spread over 11 pixels in the fluorescence image and corresponded to a bandwidth of 110 μm. By assuming a linear pH gradient across the channel, the pIs of BAS conjugate and EGFP were estimated to be around 4.6 and 5.7, respectively. The measured pI values were in good agreement with those provided by the manufacturers as 4.65 for BSA and 5.67 for EGFP.

Table 4-1

Comparisons of Focused Protein Bandwidths Obtained from the PDMS and PC Substrates with and without BSA Coating[a]

Plastic Devices	Measured Baseline Bandwidths (mm)	
	BSA Conjugate	EGFP
Unmodified PDMS	1,500[b]	1,500[b]
Precoated PDMS	200	210
Unmodified PC	1,100[b]	1,100[b]
Precoated PC	110	150

a) Experimental conditions are the same as in Fig. 4-1

b) Due to the lack of sufficient separation efficiency and resolution, only one broad protein band is observed after focusing is complete.

By assuming a Gaussian solution for the concentration distribution [86], the bandwidth of a focused analyte peak can be represented by

$$4\sigma = 4\ \{(D/E)\ [(dx/dpH)/(-d\mu/dpH)]\}^{1/2} \qquad (3\text{-}3)$$

The effect of applied electric field strength on the bandwidth of focused proteins was therefore investigated by varying the electric field from 500 to 1500 V/cm over a 1.2-cm-long PC microchannel pretreated with BSA. As summarized in Fig. 4-2A, the experimental results provided an excellent linear correlation between the measured bandwidth and $(1/E)^{1/2}$ and were in agreement with those predicted by the IEF theory in the absence of significant joule heating and protein adsorption.

Further enhancement in the separation efficiency and resolution at applied electric field strength of 1500 V/cm was evidenced by the resolution of EGFP into at least four major variants (see Fig. 4-2B) as the result of protein microheterogeneity. Such pI microheterogeneity within GFP is further supported by similar observations reported in the literature using slab gels (91) and microfluidic devices (52). The baseline bandwidth of BSA conjugate was measured to be around 70 μm inside a 1.2-cm-long PC microchannel over a pH gradient from 3 to 10. This yields to a sample concentration factor of ~170 and a baseline resolution (resolution, R_s, of 1.5) of ~ 114 peaks. Such separation and concentration performance are comparable with IEF performed over a 30-cm-long fused-silica capillary coated with a linear polyacrylamide. However, it only takes less than 45 sec for on-chip IEF at applied electric field strength of 1500 V/cm

versus 15-20 min for capillary-based protein separations. Focusing was considered to be complete when the current reached about 10% of its original value.

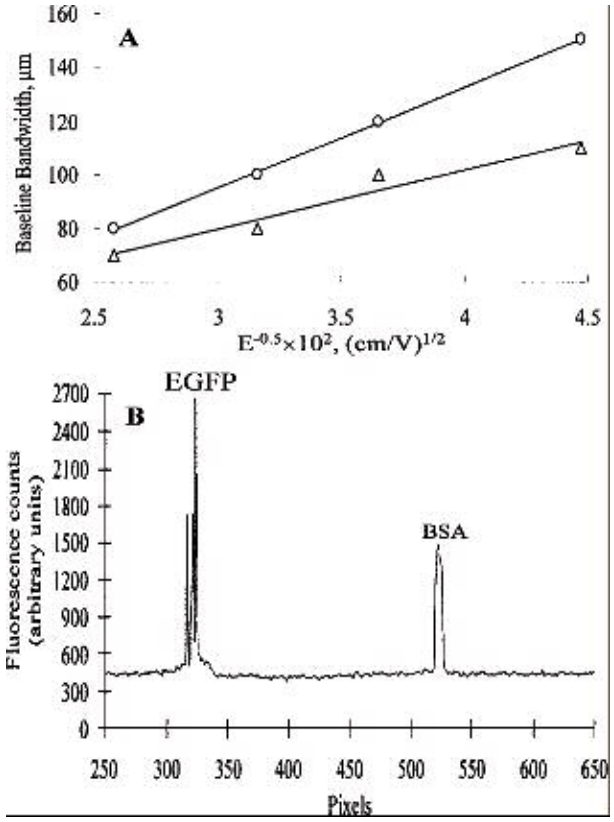

Figure 4-2 (A) Electric field strength dependence of measured protein bandwidth (Δ, BSA conjugate, R^2 = 0.95; O, EGFP, R^2 = 0.99) from PC substrate pretreated with BSA. (B) IEF separation of BSA conjugate and EGFP at constant electric field strength of 1500 V/cm in PC substrate pretreated with BSA. Other conditions are the same as in Fig. 4-1.

Dynamic Sample Introduction and Analyte Focusing in Plastic Microfluidic Devices

The dynamic approach, involving the use of electrokinetic injection of protein/peptide analytes from solution reservoirs together with simultaneous analyte focusing in the channel, was studied to significantly increase the sample loading in plastic microfluidic devices. As shown in Fig. 4-3B, the electropherogram containing resolved EGFP and fluorescein conjugated peptide of formyl-Nle-Leu-Phe-Nle-Tyr-Lys was achieved using dynamic introduction and focusing at an electric field strength of 500 V/cm for 30 min. By comparing with the electropherogram obtained using conventional IEF (see Fig. 4-3A), significant enhancements in both peak intensity and peak area were clearly demonstrated using dynamic introduction and focusing.

The baseline bandwidth of fluorescein conjugated peptide with a pI around 6.8 was considerably greater than that of EGFP (see Figs. 4-3A and 4-3B). Variation in protein/peptide bandwidth is contributed by their differences in diffusion coefficient (see Eq. 3-3). Furthermore, the effective charge of this small, fluorescein conjugated peptide approaches zero over a broad pH range rather than a narrow pH region as for proteins. Still, peptides that are most useful for characterizing and identifying proteins in proteome analysis are generally of moderate size. The focusing properties of the peptides that are of sufficient size might be expected to approach those of proteins.

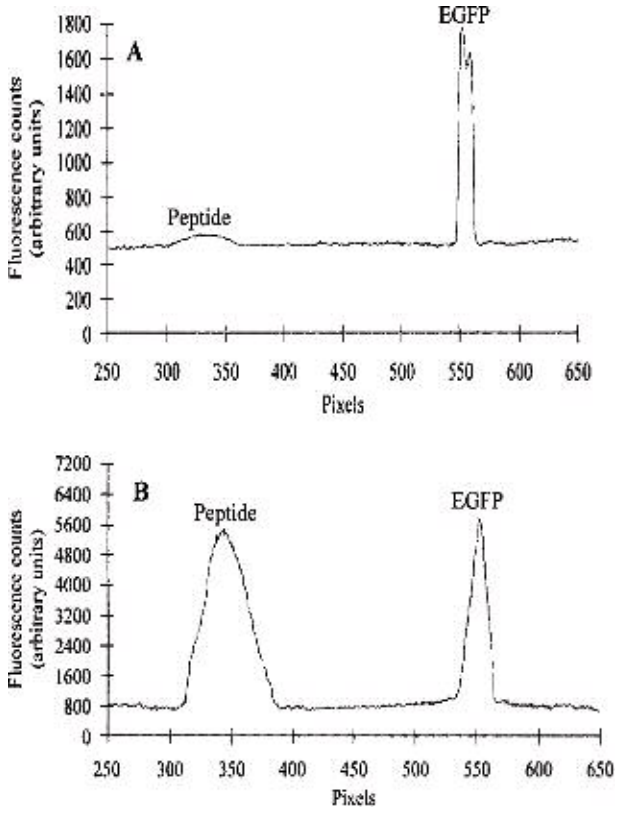

Figure 4-3 (A) Conventional IEF separation of EGFP and fluorescein conjugated peptide of formyl-Nle-Leu-Phe-Nle-Tyr-Lys using PC substrate pretreated with BSA. Sample mixture: 2% pharmalyte 3-10, 1.0 ng/mL EGFP, and 1.0 ng/mL fluorescein conjugated peptide. Other conditions are the same as in Fig. 4-1. (B) Dynamic introduction and focusing of EGFP and fluorescein conjugated peptide using PC substrate pretreated with BSA. Microchannel: 100 mm in width, 40 mm in depth, 1.2 cm in length, filled with 2% pharmalyte 3-10; anolyte: 1.0 ng/mL fluorescein conjugated peptide in 10 mM phosphoric acid (pH 2.8) and 10 mM dithiothreitol; catholyte: 1.0 ng/mL EGFP in 0.5% ammonium hydroxide (pH 10.5); injection time: 30 min; electric field strength: 500 V/cm.

For electrokinetic injection, the amount of protein/peptide introduced into the channel is controlled by the analyte's electrophoretic mobility and the injection time. Furthermore, the sample loading achieved by dynamic introduction and focusing is independent from the channel length. By maintaining constant electric field strength of 500 V/cm, dynamic introduction and focusing of EGFP and fluorescein conjugated peptide was performed using various injection times from 1 to 30 min. As shown in Fig. 4-4, the injection time dependence of peak area was presented and compared between EGFP and fluorescein conjugated peptide.

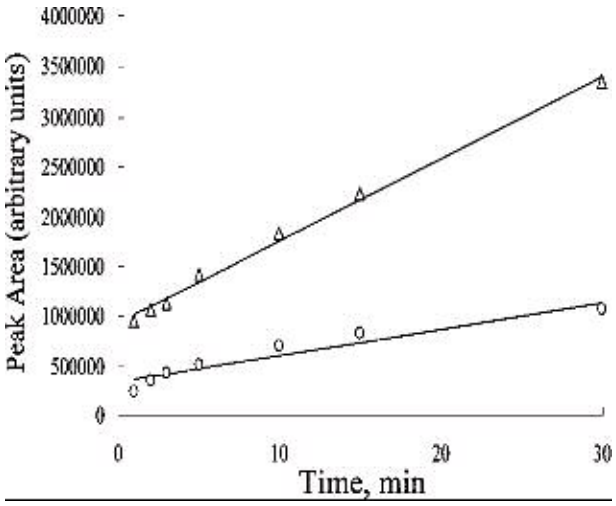

Figure. 4-4 Injection time dependence of peak area obtained from dynamic injection and focusing: D, fluorescein conjugated peptide of formyl-Nle-Leu-Phe-Nle-Tyr-Lys, R2 = 0.99; O, EGFP, R2 = 0.93. Other conditions are the same as in Fig. 4-3B. Reproducibility of peak area over four replicates at each injection time is ~6-10%

The results summarized in Fig. 4-4 clearly indicated the injection bias between EGFP and fluorescein conjugated peptide contributed by their differences in electrophoretic mobility within the sample electrophoresis buffers. For a 30 min injection time, the peak area of EGFP, corresponding to the amount of protein loading, was increased by at least one order of magnitude in comparison with conventional on-chip IEF. The peak intensity for EGFP, however, was only improved by a factor of 6 times due to the concomitant increase in bandwidth. Under the same electrokinetic conditions, the peak area of fluorescein conjugated peptide was enhanced by approximately 100 fold in comparison with conventional on-chip CIEF. The peak intensity for fluorescein

conjugated peptide, however, was only increased by a factor of 65 times due to the concomitant increase in bandwidth.

The primary focus of quantitative proteome analysis is the differential evaluation of protein expressions at various environmental conditions and physiological states. Therefore, we are not seeking absolute quantification, but rather differential measurement of the individual proteins/peptides. By employing a constant sample electrolyte solution and the identical electrokinetic conditions, differential quantification for proteome analysis would not be affected by the injection bias contributed by dynamic introduction and focusing.

4.4 CONCLUDING REMARKS

Considerable reduction in protein adsorption onto the channel wall is achieved by pretreating the plastic microfluidic devices with a BSA solution. The use of microfluidic devices is demonstrated to achieve comparable IEF separation performance as that obtained from bench-top capillary electrophoresis instruments, but at much shorter analysis time. Both the separation efficiency and resolution can be further increased by raising the applied voltage and the resultant electric field strength by assuming the absence of joule heating. Maximum achievable resolution can be obtained through voltage programming by ramping up the voltage during the focusing step, since the current decreases continuously as the result of protein focusing.

Dynamic introduction and focusing of proteins/peptides is employed to significantly enhance the sample loading and the concentrations of focused analytes in plastic microfluidic devices. Due to electrokinetic injection, the sample loading capacity

can be directly controlled by the applied electric field strength and the injection time. The observed electrokinetic injection bias is attributed to the differences in electrophoretic mobility among proteins/peptides.

Under the influence of 30 min electrokinetic injection at constant electric field strength of 500 V/cm, the sample loading achieved during dynamic introduction and focusing is estimated to be around 10-100 fold of those obtained in conventional IEF, depending on individual analyte's electrophoretic mobility. Furthermore, the sample loading during dynamic introduction and focusing is independent of channel length and only controlled by electrokinetic conditions. This channel length independence hypothesizes significant channel miniaturization with minimal loss in the sample loading for performing focusing-based electrokinetic separations using microfluidic devices.

CHAPTER 5

INTEGRATION OF ISOELECTRIC FOCUSING WITH PARALLEL SDS GEL ELECTROPHORESIS FOR MULTIDIMENSIONAL PROTEIN SEPARATIONS IN A PLASTIC MICROFLUIDIC NETWORK

5.1 INTRODUCTION

Since the concept of Micro-Total Analysis Systems (μTAS) was first proposed [1], the field has advanced rapidly, with ongoing developments promising to profoundly revolutionize modern bioanalytical methodologies. Whether termed μTAS, lab-on-a-chip, or microfluidics, the collection of technologies which define the field are proving to be an important innovation capable of transforming the ways in which bioanalytical techniques are performed. Reduced size and power requirements lead to improved portability, with higher levels of integration possible, for example on-chip micropumps for sample manipulation or liquid chromatography separations [13]. Microfabrication methods lend themselves to the formation of complex microfluidic systems, opening the way to highly parallel analytical tools, while realizing low per-unit cost for disposable applications.

Furthermore, the low volume fluid control enabled by microfluidics allows smaller dead volume and reduced sample consumption, while the low Reynolds numbers which characterize most microfluidic systems lead to highly laminar flow, eliminating the need for considering turbulent effects during instrument design. Many efficient pumping methods, including capillary action and electroosmotic flow, scale favorably in these

systems, enabling valveless flow control at the microscale. Similarly, thermal time constants tend to be extremely small due to the large surface area to volume ratio, reducing the onset of significant Joule heating during electrokinetic separations and thus allowing higher separation voltages for shorter analysis times and equivalent or better separation resolution for complex mixtures in an integrated format.

Microfluidic systems also hold great promise for realizing multidimensional separations in a single integrated system. Assuming the separation techniques used in the two dimensions are orthogonal, i.e., the two separation techniques are based on different physicochemical properties of analytes, the peak capacity of two-dimensional (2-D) separations is the product of the peak capacities of individual one-dimensional methods and can be employed for the analysis of complex mixtures [32]. To this end, several groups have explored the application of microfluidics to multidimensional peptide and protein separations. For example, Rocklin and co-workers have demonstrated 2-D separation of peptide mixtures in a microfluidic device using micellar electrokinetic chromatography and zone electrophoresis as the first and second dimensions, respectively [33]. Gottschlich et al. have also fabricated a spiral shaped glass channel coated with a C-18 stationary phase for performing reversed-phase chromatographic separation of trypsindigested peptides [34]. By employing a cross interface, the eluted peptides from the micellar electrokinetic chromatography [33] or reversed-phase chromatography channel [34] were sampled by a rapid zone electrophoresis separation in a short glass microchannel. Additionally, Herr and co-workers have coupled isoelectric focusing (IEF) with zone electrophoresis for 2-D separations of model proteins using plastic microfluidics [27].

In each of these examples, the multiple separation dimensions are performed serially, without the ability to simultaneously sample all proteins or peptides separated in the first dimension for parallel analysis in the second dimension. As an early step toward this goal, a microfabricated quartz device has been proposed by Becker and co-workers with a single channel for the first dimension and an array of 500 parallel channels with submicron dimensions as the second dimension positioned orthogonally to the first dimension channel [35]. In a further step, Chen et al. recently described a 2-D capillary electrophoresis system based on a 6-layer poly(dimethylsiloxane) (PDMS) microfluidic system [26]. The system consisted of a 25 mm-long microchannel for performing IEF, with an intersecting array of parallel 60 mm-long microchannels for achieving sodium dodecyl sulfate-polyacrylamide gel electrophoresis (SDS-PAGE). This 6-layer PDMS microfluidic device, however, required the alignment, bonding, removal, re-alignment, and re-bonding of various combinations of the six layers to perform a full 2-D protein separation.

It should be emphasized that the extremely high resolution of 2-D PAGE for protein separation is mostly contributed by IEF under denaturing conditions in the first separation dimension. Attempts to perform native 2-D electrophoresis results in 2-D protein patterns with poor reproducibility, smears, and less distinct protein spots [92]. In this work, nonnative IEF is therefore chosen for the first separation dimension and carried out in a single-layer 2-D microfluidic network fabricated in a rigid polymer substrate. Once the focusing is complete, the focused proteins are simultaneously transferred using an electrokinetic method from the first dimension microchannel into an array of second

dimension microchannels for achieving parallel size-dependent separations on each sampled fraction of focused proteins using SDS gel electrophoresis. The use of nonnative IEF further prepares denatured protein analytes for rapid and effective formation of SDS-protein complexes required for performing electrokinetic transfer between the coupled separation dimensions and SDS gel electrophoresis.

5.2 EXPERIMENTAL SECTION

Materials and Reagents

Fluorescent protein conjugates summarized in Table 5-1 and SYPRO Red were purchased from Molecular Probes (Eugene, OR). Pharmalyte 3-10 was acquired from Amersham Pharmacia Biotech (Uppsala, Sweden). Tris(hydroxymethyl)-aminomethane (Tris) and ultrapure urea were obtained from Bio-Rad (Hercules, CA). All other reagents, including ammonium hydroxide, bovine serum albumin, dithiothreitol (DTT), fluorescein, hydrofluoric acid, iodoacetamide (IAM), phosphoric acid, polyethylene oxide (PEO, average MW 600,000), potassium hydroxide, and SDS, were acquired from Sigma (St. Louis, MO). All aqueous solutions were prepared using water purified by a Nanopure II system (Dubuque, IA) and further filtered with a 0.22 μm membrane (Costar, Cambridge, MA).

Table 5-1

List of Model Proteins (Conjugated with Fluorescein) Employed in this Study

Proteins	Reported pI[a]	Distance from Focused Protein Band to Reservoir B (cm)	Calculated pI[b]	Molecular Mass
Parvalbumin	4.10	0.14	3.98	12.3 kDa
Ovalbumin	4.50	0.23	4.61	45 kDa
Trypsin Inhibitor	4.55	0.23	4.61	21.5 kDa
Bovine Serum Albumin	4.60	0.23	4.61	66 kDa
Actin	5.20	0.33	5.31	43 kDa

a) The pI values were provided by Molecular Probes.

b) The pI values were calculated using pI = 3 + (distance from focused protein band to reservoir B x 7.0 pH units/cm).

Protein Sample Preparation

Each model protein (Table 5-1) with a concentration of 1mg/mL was completely denatured and reduced in a 100 mM Tris buffer (pH 8.0) containing 8 M urea and 0.1 M DTT for 2 hr at 37 °C under a nitrogen atmosphere. Proteins were alkylated to maintain their reduced states during the IEF separations by adding excess IAM with a final concentration of 50 mM. The reaction was allowed to proceed for 30 min at room temperature in the dark. A PD-10 size exclusion column (Amersham Pharmacia Biotech)

was employed for buffer exchange and proteins were eluted in a solution containing 10 mM Tris at pH 8.0.

Fabrication of Plastic Microfluidic Network

The fabrication of a silicon template was performed by following standard procedure involving photolithography and chemical etching. Briefly, the template starting substrate consisted of a 10 cm diameter <100> oriented p-type silicon wafer coated with 2.4 μm of thermally grown silicon dioxide (WaferNet, San Jose, CA). Standard photolithography was performed using a transparency film mask and a contact mask aligner to pattern inverse microchannel features into a thin layer of photoresist. The wafer was then placed in a 5:1 buffered hydrofluoric acid solution to remove the exposed silicon dioxide. The remaining silicon dioxide was then used as a hard mask for silicon patterning, allowing the bulk wafer to be etched anisotropically in 45% (w/v) potassium hydroxide solution to form a positive relief mold containing three-dimensional structures for fabrication of the desired plastic microchannel designs.

Polycarbonate (PC) disks, 9.0 cm in diameter, were cut from a 1.5 mm thick PC sheet (Sheffield Plastic, Sheffield, MA) for imprinting microchannels with the silicon template. The PC substrate was placed over the silicon template and the whole assembly was sandwiched between two glass plates. A hydraulic press was employed to apply a pressure of 300 psi at 160 °C for 5 min. After the pressure was released, the PC substrate containing imprinted microchannels was cooled down and subsequently removed from the press. The open microchannels were aligned with another PC substrate containing drilled holes for fluid access. To achieve thermal bonding between two PC substrates, the

whole assembly was again sandwiched between two glass plates and placed inside the press under 900 psi and 138 °C for 10 min, creating an irreversible seal for the microchannels. The surface of the device retained optical quality following the thermal bonding step. The entire fabrication process was performed in a class-1000 cleanroom to prevent any particulate contamination of the polymer microfluidic device.

The 2-D plastic microfluidic network employed for rapidly separating protein analytes with high resolution based on their differences in isoelectric point (pI) and molecular mass is shown conceptually in Fig. 5-1. The newly fabricated devices were cleaned with methanol and rinsed with 10 mM Tris at pH 8.0 for 10 min. To reduce protein adsorption, the PC substrates were flushed with a bovine serum albumin solution (5 mg/mL in 10 mM Tris at pH 8.0) prior to performing 2-D protein separations.

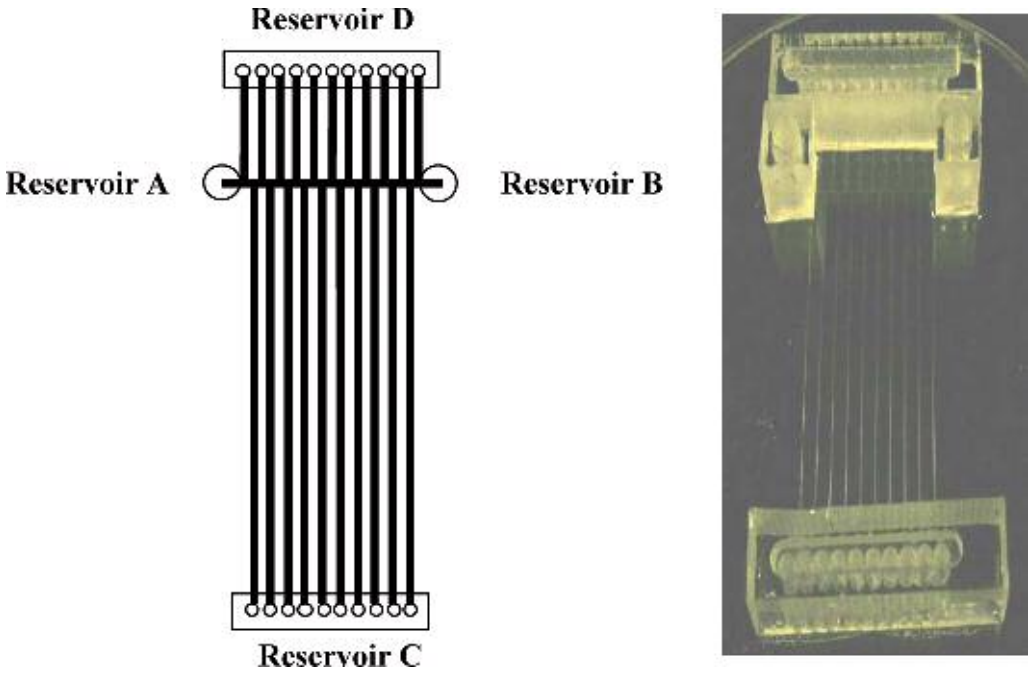

Figure 5-1 Schematic and image of 2-D protein separation platform using plastic microfluidics.

2-D Protein Separations Using Single Separation Medium

Two different approaches, including the introduction of single or multiple separation media into microfluidic network, were employed to study the optimization of 2-D protein separations. For the first approach, the PC device was filled with a gel solution containing 1.5% PEO and 2% pharmalyte 3-10. A dynamic introduction and focusing method demonstrated in previous studies [49] was utilized for only introducing protein analytes into the first separation dimension provided by the microchannel (1 cm in length, 100 μm in width and 40 μm in depth) connecting reservoirs A and B (see Fig. 5-1). Briefly, a mixture of protein-fluorescein conjugates (see Table 5-1), which were denatured, reduced, and alkylated, was prepared using the catholyte solution (30 mM ammonium hydroxide at pH 10.5) with a final concentration of 10 ng/μL for each model protein and placed in reservoir A. A solution of 10 mM phosphoric acid at pH 2.8 was employed as the anolyte and placed in reservoir B. Sample loading and protein focusing were performed at an electric field of 500 V/cm for 90 s using a CZE 1000R high-voltage power supply (Spellman High-Voltage Electronics, Plainview, NY).

The separation voltage was turned off as soon as the dynamic protein introduction and focusing was complete in the IEF microchannel. Reservoir D (see Fig. 5-1) was then filled with a 10 mM Tris buffer containing 2% SDS. A positive voltage to create an electric field of 500 V/cm between reservoirs C and D was applied at reservoir C for 30 s for rapid electrokinetic injection and filling of SDS within the IEF microchannel, followed by the incubation of focused proteins with SDS for 5 min. Since non-native IEF was used as the first separation dimension, SDS-protein complexes formed very rapidly while avoiding significant diffusion band broadening of focused proteins. Additionally,

the high viscosity of the gel medium also restricted diffusional band broadening during the incubation process. The rapid formation of SDS-protein complexes not only established the foundation for performing electrokinetic protein transfer, but also prepared protein analytes for size-based separation in the second dimension.

All model proteins resolved in the second separation dimension were monitored using non-covalent, environment-sensitive, fluorescent probes such as SYPRO Red (excitation: 550 nm; emission: 630 nm) [93]. To introduce the probes, the 2% SDS solution originally present in reservoir D (Fig. 5-1) was replaced with a 10 mM Tris buffer containing 0.05% SDS and 1X SYPRO Red. The newly-labeled negatively charged SDS-protein complexes were then electrokinetically injected into the lower microchannel array by applying a positive electric field of 500 V/cm from reservoir C to reservoir D, with reservoirs A and B electrically floating. Using this approach, each plug of focused proteins residing in the IEF microchannel between a given pair of adjacent upper channels was electrokinetically injected into its corresponding second separation dimension microchannel (4 cm in length, 100 μm in width and 40 μm in depth). Sizebased protein separation was measured using a Nikon fluorescence microscope (Melville, NY), which was equipped with a high sensitivity charge-coupled device camera from Andor Technology (Belfast, Northern Ireland).

2-D Protein Separations Using Multiple Separation Media

IEF involved the use of carrier ampholytes for the creation of a pH gradient in the microchannel. However, the size-dependent separation of SDS-protein complexes was based on their differences in electrophoretic mobility inside a polymer-sieving matrix. Instead of using a single gelbased separation medium, the ability to introduce and isolate

two different separation media in the 2-D plastic microfluidic network was developed using a pressure filling method and employed for achieving optimal separation performance. The entire PC device was initially filled with a 1.5% PEO solution. An aqueous solution containing protein analytes and 2% Pharmalyte 3-10 was introduced into the IEF microchannel from reservoir B using pressure while reservoirs C and D were completely sealed (see Fig. 5-1). The gel/solution interface at the intersections of the microchannel array and the channel connecting reservoirs A and B was monitored by adding fluorescein into the PEO solution and using a Nikon fluorescence microscope (Melville, NY) equipped with a computer controlled moving stage. The filling was stopped as soon as the aqueous solution reached reservoir A. The solutions of 10 mM phosphoric acid (pH 2.8) and 30 mM ammonium hydroxide (pH 10.5) were added into reservoirs B and A and employed as the anolyte and the catholyte, respectively. Protein focusing was performed at an electric field of 500 V/cm for 90 s, followed by SDS-protein complexation, electrokinetic transfer, SYPRO Red labeling, and size-based protein separation using the same procedures as described previously.

5.3 RESULTS AND DISCUSSION

An important aspect of any multidimensional separation platform is its ability to improve the detection of analytes present in low quantities during the analyses of complex protein mixtures. The use of IEF as the first separation dimension provides excellent resolving power with a typical concentration factor of 50-100 times. Pretreatment of the PC devices resulting in the adsorption of bovine serum albumin and carrier ampholytes onto the plastic channel walls eliminates the electroosmotic flow. This

is evidenced by the lack of movement of focused protein bands after the focusing is complete. The lack of electroosmosis in chip-based IEF separations is further supported by the previous work using PC and PDMS devices pretreated with bovine serum albumin [49].

The typical protein bandwidth after focusing was around 130 μm inside a 1-cm long IEF microchannel by applying electric field strength of 500 V/cm over a pH gradient from 3 to 10 (see Fig. 5-2A). This yielded to a baseline resolution of ~80 peaks or pI difference as small as 0.09 pH units. By comparing with the results obtained from single IEF separations with peak capacities of approximately 30-50 (22,94,95), the combined usage of a PC substrate with the bovine serum albumin pretreatment offers improvement in separation resolution. Further enhancement in separation resolution can be achieved by raising the applied voltage or using carrier ampholytes in support of narrow pH gradients [86].

2-D Protein Separations Using Single Separation Medium

Dynamic protein introduction and focusing (10) was employed to achieve sample loading in PC devices filled with a single separation medium containing 1.5% PEO and 2% pharmalyte 3-10. Protein-fluorescein conjugates present in reservoir A (see Fig. 5-1) continuously migrated into the IEF microchannel and encountered a pH gradient established by carrier ampholytes originally present in the channel for focusing and separation. Thus, the sample loading during dynamic sample introduction and analyte focusing is no longer dependent on channel length, but is instead controlled only by electrokinetic conditions, including the injection time and the applied electric field strength. This channel length independence hypothesizes the potential for significant

channel miniaturization with minimal loss in the sample loading for performing focusing-based electrokinetic separations using microfluidic devices.

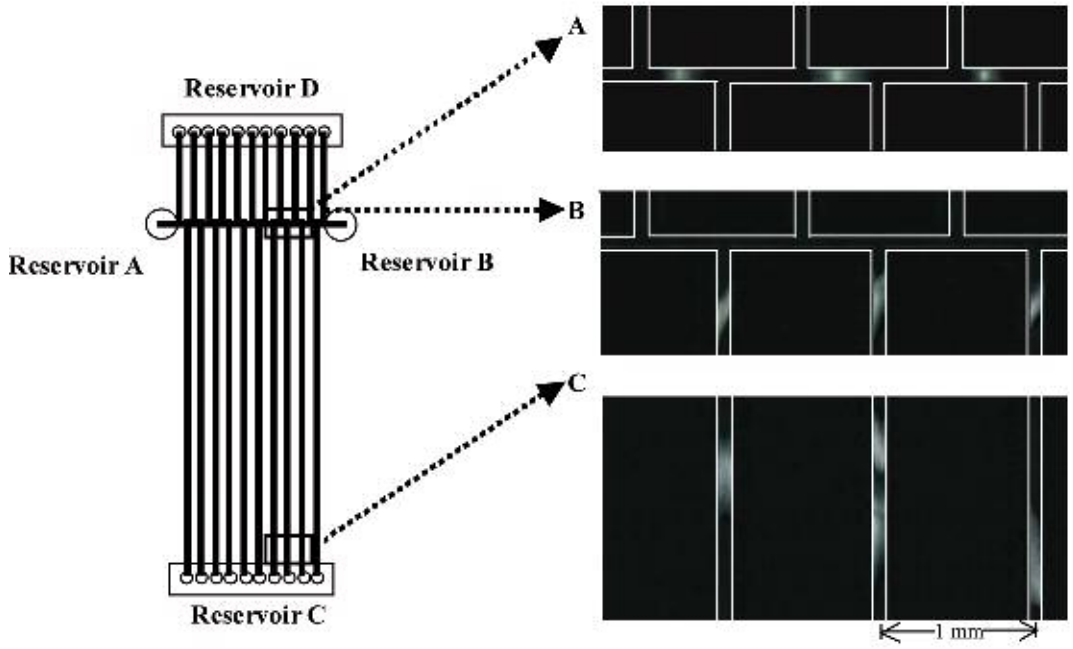

Figure 5-2 Fluorescent images of on-chip 2-D separation of four model proteins using single separation medium. (A) non-native IEF with focusing order of (i) actin, (ii) bovine serum albumin and trypsin inhibitor, and (iii) parvalbumin from left to right; (B) electrokinetic transfer of focused proteins; (C) SDS gel electrophoresis. Images were captured at either 90 s or 150 s following the initiation of IEF or SDS gel electrophoresis separations, respectively. Images were obtained using either green fluorescence of protein-fluorescein conjugates in IEF or red fluorescence of SYPRO Red labeled proteins during electrokinetic transfer and size-based separation.

Four model proteins consisting of parvalbumin (pI 4.10, MW 12.3 kDa), trypsin inhibitor (pI 4.55, MW 21.5kDa), bovine serum albumin (pI 4.60, MW 66 kDa), and actin (pI 5.20, MW 43.0 kDa) were employed for early demonstration of 2-D separations in the plastic microfluidic network. To fulfill the requirements of a comprehensive 2-D separation system, any separation accomplished by the first dimension should ideally be retained upon transfer to the second dimension. To achieve this goal, an electrokineticbased technique was demonstrated for successfully transferring focused proteins from the IEF microchannel into the second separation dimension (see Fig. 5-2B). The transfer process was facilitated by designing the microfluidic network such that the upper and lower second dimension channels were arranged in a staggered configuration (see Fig. 5-1). This configuration allowed for the entire contents of the first dimension IEF channel between the two outermost channels of the upper second dimension array to be transferred into channels of the lower second dimension array in a single process (see Fig. 5-3). A key benefit of this approach lies in its ability to minimize band broadening during the transfer. Still, initial studies with simple right-angle intersections such as those depicted in Fig. 5-2B have been found to result in approximately 1.5-2x broadening of focused protein bands during transfer. The extent of band broadening during the transfer step is largely dependent upon the electric field distribution within the intersection region, in combination with variations in total path length traveled by proteins at different locations within the intersection.

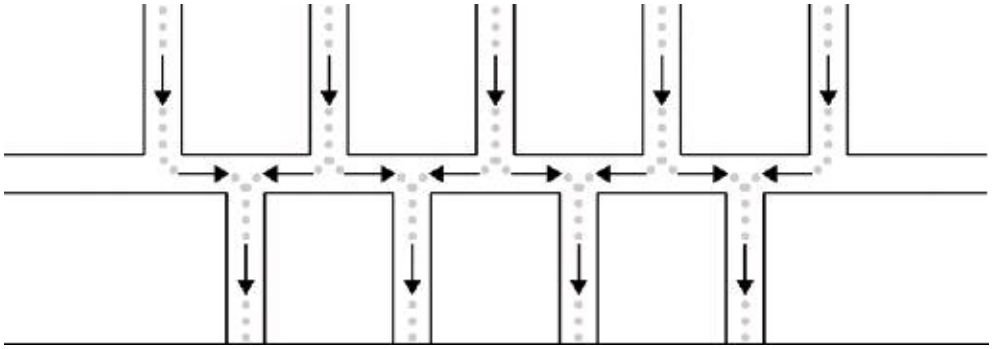

Figure 5-3 Schematic depicting the paths for electrokinetic introduction of SDS from reservoir D (see Fig. 5-1) to microfluidic network and electrokinetic transfer of focused protein bands between the first and second separation dimensions.

Through the use of electrokinetic transfer, the extent of urea and focused ampholytes transferred from the first to second separation dimensions is extremely low due to the lack of net charge in both urea and focused ampholytes. Furthermore, the presence of minimal amounts of urea and ampholytes are not expected to have any significant effects on the size-based separation in the second dimension microchannels. It is well known that the extremely high resolution of 2-D PAGE is mostly contributed by IEF under denaturing conditions. The urea utilized for protein denaturation during the sample preparation and remaining during SDS incubation exhibits essentially no impact in IEF and SDS-PAGE separations.

It has been reported that the formation of SDS-protein complexes is the critical step in determining separation resolution of capillary gel electrophoresis [31]. Once the SDSprotein complexes are properly formed, they remain relatively stable and the presence of SDS in the separation buffer is no longer needed for further stabilization.

This is particularly true for rapid protein separation in capillary gel electrophoresis and microfluidics-based devices. Thus, a 2% SDS solution was employed and electrokinetically introduced into the IEF channel for complexation with focused proteins. The SDS-protein complexation was allowed to proceed for 5 min. Shorter reaction times may result in incomplete SDS binding to the proteins and longer incubation times may contribute to additional protein band broadening due to diffusion.

Instead of using green fluorescence of protein-fluorescein conjugates for acquiring the images of focused protein bands (see Fig. 5-2A), protein analytes migrated within the intersection region (see Fig. 5-2B) and resolved during the size-based separation (see Fig. 5-2C) were monitored using non-covalent, environment-sensitive, fluorescent probes such as SYPRO Red (11). As shown in Fig. 5-2A, the first dimension focusing was unable to resolve trypsin inhibitor and bovine serum albumin with a pI difference of only 0.05 pH unit. However, following transfer to the second dimension and size-based separation, all four model proteins were successfully resolved.

The SYPRO Red probes are non-fluorescent in water but highly fluorescent in detergent, in which they take advantage of SDS binding to proteins to build a fluorescence-promoting environment. In comparison with covalently labeling proteins, the use of SYPRO staining not only presents a generic detection approach for the analysis of complex protein mixtures such as cell lysates, but also avoids additional introduction of protein microheterogeneity as the result of labeling reaction. However, SDS concentration in the electrophoresis buffer has a significant effect on protein labeling using SYPRO dyes. When the SDS concentration is above its critical micellar concentration, 8.3 mM (~0.24% in water and somewhat less in buffer solutions), the

major portion of the staining dye attaches to the SDS micelles instead of the SDS-protein complexes.

In order to efficiently and rapidly label SDS-protein complexes using SYPRO dyes and to sensitively detect the resolved SDS-protein complexes, Csapo and co-workers [96] have determined the optimal SDS concentration in the electrophoresis buffer to be around 0.05%. Their results were confirmed in previous studies and further supported by the work of Bousse et al. [30], in which an on-chip SDS dilution step was required between the separation channel and laser-induced fluorescence detection. The dilution step reduced the SDS concentration from 0.25 to ~ 0.025%. Such dilution thus broke up the SDS micelles, thereby allowing more dye molecules to bind to the SDS-protein complexes. This rearrangement prior to the fluorescence detection led to an increase in the peak amplitude by one order of magnitude.

Furthermore, comparison of SYPRO dyes with silver staining in SDS gels has shown that this class of fluorescent dyes detects polypeptides with sensitivity similar to that obtained by silver staining [93,97,98]. Binding of the dyes to the protein is stoichiometric and fluorescence is related to the amount of dye binding, therefore, the dynamic range is three orders of magnitude greater than for silver staining [97]. The current protein detection sensitivity, involving the use of a fluorescence microscope, is approximately 0.5 ng/μL. This can be further reduced by using the dynamic introduction and focusing approach as demonstrated in previous studies [49]. Finally, it has been shown that proteins detected by SYPRO staining are compatible with matrix-assisted laser desorption/ionization mass spectrometry analysis [98,99].

2-D Protein Separations Using Multiple Separation Media

In this work, a two-step pressure filling method has been developed to introduce and isolate two different separation media in the 2-D plastic microfluidic network. The filling process was monitored by adding fluorescein into the PEO gel solution and using a fluorescence microscope equipped with a computer controlled moving stage. The fluorescent image of gel/solution interface (see Fig. 5-4) at the intersections of the IEF microchannel and the microchannel array illustrated the capability for introducing multiple separation media, including the ampholyte solution containing protein analytes and the PEO gel required for performing IEF and size-based separations, respectively. While a slight degree of diffusion by small molecules such as fluorescein/ampholyte was evident in the microchannels, conventional IEF separations performed in the first dimension microchannel exhibited negligible degradation of separation resolution due to the limited protein diffusion and the zone sharpening effect which occurred during IEF (see Fig. 5-5A). Further increase in sample loading can be achieved using dynamic analyte introduction and focusing as reported previously [49] and employed in PC devices containing a single separation medium.

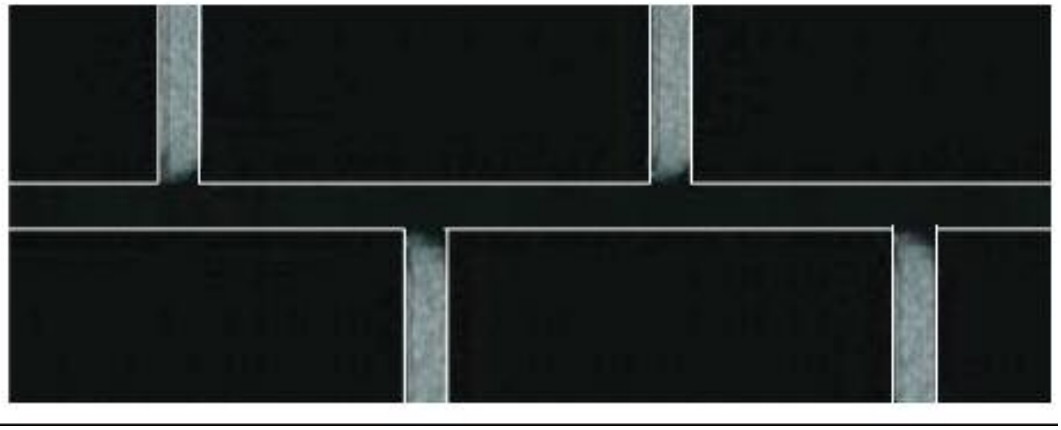

Figure 5-4 Image of plastic microfluidic network filled with multiple separation media.

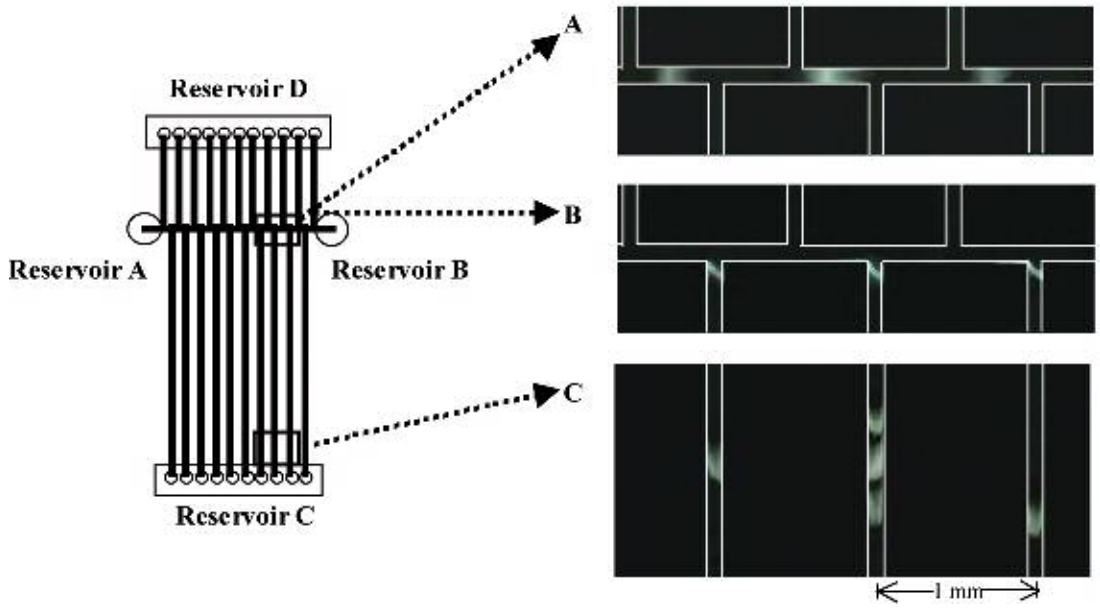

Figure 5-5 Fluorescent images of on-chip 2-D separation of five model proteins using multiple separation media. (A) non-native IEF with focusing order of (i) actin, (ii) bovine serum albumin, ovalbumin, and trypsin inhibitor, and (iii) parvalbumin from left to right; (B) electrokinetic transfer of focused proteins; (C) SDS gel electrophoresis. Images were captured at 90 s following the initiation of IEF or SDS gel electrophoresis separations. Images were obtained using either green fluorescence of protein-fluorescein conjugates in IEF or red fluorescence of SYPRO Red labeled proteins during electrokinetic transfer and size-based separation.

In analogy to stacking gel as employed in SDS-PAGE, the gel/solution interface in the microfluidic system provides a mechanism for protein stacking during electrokinetic transfer between the coupled separation dimensions (see Figs. 5-5A and 5-5B). Instead of acquiring additional band broadening as observed when using a single separation medium (see Figs. 5-2A and 5-2B), the bandwidth of focused proteins was

reduced by approximately a factor of 2 as the result of protein stacking at the gel/solution interface. By reducing the size of the injected bandwidth in the second dimension, significant enhancement in sizebased resolving power was evident for baseline resolution of bovine serum albumin, ovalbumin, and trypsin inhibitor (see Fig. 5-5C). It should be noted that the length of lower microchannel array was reduced from 4 cm in the single separation medium case to 2.5 cm when using multiple separation media. Furthermore, the standard curves for molecular mass estimation were constructed by plotting the logarithmic molecular masses of model proteins examined in this study against their migration distances from the intersections measured during SDS gel electrophoresis (see Figs. 5-2C and 5-5C). As shown in Fig. 5-6, a good linear correlation was demonstrated in both SDS gel electrophoresis studies over the range of 12.3 to 66 kDa.

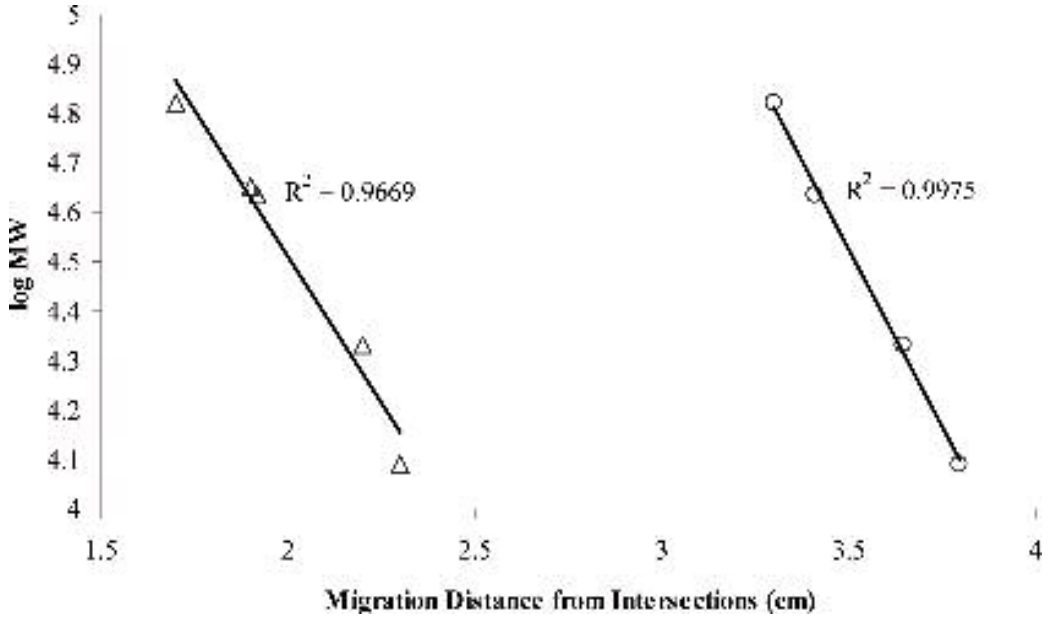

Figure 5-6 Standard curves of logarithmic molecular mass versus migration distance from intersections during SDS gel electrophoresis studies performed using single (○) or multiple (□) separation media. These migration distances were taken from the images presented in Figs. 5-2C and 5-5C.

A comprehensive 2-D protein separation was completed in less than 10 min, with the majority of time consumed in the required SDS-protein complexation reaction. Furthermore, a peak capacity of ~170 in the second dimension of size-based separation was estimated by assuming average bandwidth of 150 μm over a span of 2.5 cm channel length. Further improvements in peak capacity may be realized using longer channels in larger chips during the size-based separation. Because the separation mechanisms in IEF and SDS-PEO gel electrophoresis were completely orthogonal, the overall peak capacity in the current 2-D protein separation platform was anticipated to be around 1,700 (10 fractions from IEF x 170 from SDS-PEO gel electrophoresis). Significant enhancement in the peak capacity of the multidimensional separation platform can be realized by further raising the density of microchannels in the array, thereby increasing the number of IEF fractions analyzed in the size-based separation dimension. Due to the use of parallel separations in the second dimension, there is no accompanying increase in the analysis time.

5.4 CONCLUSION

The demonstrated on-chip combination of non-native IEF with SDS-PEO gel electrophoresis offers electrokinetic focusing for concentrating dilute protein samples while providing excellent resolving power in a multidimensional separation platform. Instead of sequentially sampling and analyzing eluants from the first separation dimension as previously reported in the literature [27,33,34], an electrokinetic transfer technique is employed to simultaneously introduce all the focused protein bands from the first to second separation dimensions, enabling parallel and high throughput size-based

separation in a solution containing SDS and PEO sieving matrix. The ability to introduce and isolate multiple separation media in the plastic microfluidic network further provides protein stacking during electrokinetic transfer between the coupled separation dimensions.

The single-layer 2-D microfluidic network fabricated in a PC substrate not only allows straightforward implementation and automation of multidimensional protein separations in a low-cost disposable platform, but also provides excellent resolving power toward the analysis of complex protein mixtures. A comprehensive 2-D protein separation is completed in less than 10 min with an overall peak capacity of around 1,700. The reproducibility of this technology can be further improved upon by the development of an automated system capable of performing all processes involved in the analysis in an autonomous fashion. Furthermore, the resolving power and sensitivity of the analysis can be greatly enhanced by utilizing microfluidic networks containing a higher density of second dimension channels as well as employing more sensitive multichannel laser-induced fluorescence detection systems such as those previously reported in the literature [100,101]. Ultimately, this work demonstrates the potential for microfluidic technology to transform conventional 2-D PAGE into an automated, portable, rapid, and reproducible protein bioanalytical technology.

CHAPTER 6

CONCLUSION

This dissertation first summarizes a subset of the underlying microfabrication methods which are enabling new analytical tools, and then describes the state-of-the-art developments in some key areas of proteome analysis in microfluidic systems. Ongoing developments in microfluidics technology are leading to novel bioanalytical tools which are beginning to have a profound impact on the field of proteomics. Beyond microarray-based immunoassay platforms, microfluidic systems hold the promise of greatly enhanced performance and automation for a range of proteomics applications, in addition to higher levels of integration and portability which are the hallmark of microfabricated devices. These emerging microfluidics tools offer capabilities to improve the speed, repeatability, reliability, and range of protein analysis, by addressing the key issues and bottlenecks in existing bench-top analytical methods, and present the vision of bringing proteomic analysis to a comparable level of efficiency as currently exists for its genomic counterpart.

On-line coupling of a μ-trypsin membrane reactor with miniaturized membrane chromatography is investigated as an integrated microanalytical tool. The combination of rapid protein digestion, high-resolution peptide separation, and sensitive protein identification using ESI-MS not only reduces sample consumption, dead volume and the elution times in miniaturized membrane chromatography, but also enhances the dynamic range and the detection sensitivity in the proteomic analysis.

To further enhance the separation performance of a protein/peptide mixture, an isoelectric focusing separation is achieved on a single dimensional microfluidic channel

by pretreating the plastic device with a protein solution to reduce protein adsorption. The use of microfluidic device shortens the analysis time and demonstrates comparable IEF separation efficiencies as that obtained from bench-top instruments. Moreover, separation resolution can be increased by raising the applied voltage and the electric field strength due to the better heat dissipation ability in minimized separation platform.

In conventional IEF separation, the entire channel is filled with a solution mixture containing protein/peptide analytes and carrier ampholytes for the creation of a pH gradient. The limited injection volume is a more critical issue for on-chip separation even than capillary IEF. To increase sample loading, a dynamic approach, which is based on electrokinetic injection of proteins/peptides from solution reservoirs instead of microchannels is studied at on-chip IEF. The proteins/peptides continuously migrate into the plastic microchannel and encounter a pH gradient established by carrier ampholytes originally present in the channel for focusing and separation. Under the 30 min electrokinetic injection at constant electric field strength of 500 V/cm, the sample loading of a protein/peptide mixture is enhanced by approximately 10-100 fold in comparison with conventional isoelectric focusing. The capacity of protein/peptide loading can be directly controlled by the injection time and the applied electric field strength. Differences in the sample loading are contributed by electrokinetic injection bias and are affected by the electrophoretic mobility among individual analyte.

Furthermore, a single-layer 2-D microfluidic network is demonstrated for rapidly separating protein analytes with ultrahigh resolution based on their differences in pI and molecular weight. Briefly, the first dimensional microchannel is employed for performing a non-native IEF separation. Once the focusing is complete, the focused proteins are

simultaneously transferred using an electrokinetic method into the 10 orthogonal microchannel array connected with the focusing microchannel for performing a parallel and high throughput size-dependent separation. The transferred proteins are first incubated and complexed with SDS and non-covalent, environment-sensitive, fluorescent probes of SYPRO Red. The protein complexes are then separated in the microchannel array containing a replaceable polymer sieving matrix and measured using a fluorescence microscope.

As an initial demonstration of the system, four model proteins are separated in a test chip with 100 mm wide microchannels. The first dimension focusing is unable to resolve two proteins that have a pI difference of only 0.05 pH unit. However, following transfer to the second dimension and size-based separation are successfully resolved all four model proteins. The separation of more complex samples has also been demonstrated using a multidimensional system. The ability to introduce and isolate multiple separation media in plastic microfluidic network is one key requirement for achieving multidimensional protein separations. Five proteins have been successfully separated based on this approach. The focused protein bands stacking on the multimedia interface enhances the separation resolution at the second dimension due to reducing the initial bandwidth in the size-based gel electrophoresis.

A comprehensive 2-D protein separation is completed in less than 10 min with an overall peak capacity of around 1,700 using this chip with planar dimensions of as small as 2cm x3cm. Significant enhancement in the peak capacity can be realized by raising the density of microchannels in the array, thereby increasing the number of IEF fractions analyzed in the size-based separation dimension.

Although this simple study involved a limited number of second dimension microchannels, the ability for a microfluidic platform to perform parallel 2-D separations of complex protein samples has been demonstrated. Furthermore, microfabricated systems have the potential to automate and combine high throughput multidimensional protein separations in a microfluidic network that are readily available in the macroscopic world.

APPENDICES

I. Chapter 2 is published on *Journal of Chromatography A*, 979 (2002) 241-247

"Miniaturized Membrane-Based Reversed-Phase Chromatography and Enzyme Reactor for Protein Digestion, Peptide Separation, and Protein Identification Using Electrospray Ionization Mass Spectrometry"

Yan Li[1], Jonathan W. Cooper[1], Cheng S. Lee[1]

II. Chapter 3 is published on *Electrophoresis* 2003, 24, 193–199

"Dynamic Analyte Introduction and Focusing in Plastic Microfluidic Devices for Proteomic Analysis"

Yan Li[1], Donald L. DeVoe[2], Cheng S. Lee[1]

III. Chapter 3 is submitted to *Analytical Chemistry* for publication

"Integration of Isoelectric Focusing with Parallel SDS Gel Electrophoresis for Multidimensional Protein Separations in A Plastic Microfluidic Network"

Yan Li[1], Jesse S. Buch[1], Frederick Rosenberger[3], Donald L. DeVoe[2], Cheng S. Lee[1]

[1] Department of Chemistry and Biochemistry
University of Maryland, College Park, MD 20742

[2] Department of Mechanical Engineering and Institute for System Research
University of Maryland, College Park, MD 20742

[3] Calibrant Biosystems, 7507 Standish Place, Rockville, MD 20855

REFERENCES

1. Manz, A., Graber, N., and Widmer, H. M. (1990). "Miniaturized total chemical analysis systems: a novel concept for chemical sensing," *Sensors and Actuators* B1, 244-248.

2. Soper, S. A., Ford, S. M., Qi, S., McCarley, R. L., Kelly, K., and Murphy, M. C. (2000). "Polymeric microelectromechanical systems," *Anal. Chem.* 72, 643A-651A.

3. Martynova, L., Locascio, L. E., Gaitan, M., Kramer, G. W., Christensen, R. G., and MacCrehan, W. A. (1997). "Fabrication of plastic microfluidic channels by imprinting methods," *Anal. Chem.* 69, 4783-4789.

4. Xu, J., Locascio, L. E., Gaitan, M., and Lee, C. S. (2000). "Room-temperature imprinting method for plastic microchannel fabrication," *Anal. Chem.* 72, 1930-1933.

5. Rosenberger, F., Jones, E., Lee, C. S., and DeVoe, D. L. (2002). "High pressure thermal bonding for sealing of plastic microstructures," *Proceedings of the Micro Total Analysis Systems*, Kluwer Academic Publishers, pp. 404.

6. Jackman, R. J., Wilbur, J. L., and Whitesides, G. M. (1995). "Fabrication of submicrometer features on curved substrates by microcontact printing," *Science* 269, 664-666.

7. Duffy, D. C., McDonald, J. C., Schueller, J. A., and Whitesides, G. M. (1998). "Rapid prototyping of microfluidic systems in poly(dimethylsiloxane)," *Anal. Chem.* 70, 4974-4984.

8. McDonald, J. C., Duffy, D. C., Anderson, J. R., Chiu, D. T., Wu, H., Schueller, O. J. A., and Whitesides GM (2000). "Fabrication of microfluidic systems in poly(dimethylsiloxane)," *Electrophoresis* 21, 27-40.

9. Oleschuk, R. D., Shultz-Lockyear, L. L., Ning, Y., and Harrison, D. J. (2000). "Trapping of bead-based reagents within microfluidic systems, on-chip solid-phase extraction and electrochromatography," *Anal. Chem.* 72, 585-590.

10. Ericson, C., Holm, J., Ericson, T., and Hjerten, S. (2000). "Electroosmosis- and pressure-driven chromatography in chips using continuous beds," *Anal. Chem.* 72, 81-87.

11. He, B., Tait, N., and Regnier, F. (1998). "Fabrication of nanocolumns for liquid chromatography," *Anal. Chem.* 70, 3790-3797.

12. Throckmorton, D. J., Shepodd, T. J., and Singh, A. K. (2002). "Electrochromatography in microchips, reversed-phase separation of peptides and amino acids using photopatterned rigid polymer monoliths," *Anal. Chem.* 74, 784-789.

13. Harris, C. M. (2003). "Shrinking the LC landscape," *Anal. Chem.* 75, 65A-69A.

14. Figeys, D., and Pinto, D. (2001). "Proteomics on a chip, promising developments," *Electrophoresis* 22, 208-216.

15. Liu, Y. J., Foote, R. S., Culbertson, C. T., Jacobson, S. C., Ramsey, R. S., and Ramsey, J. M. (2000). "Electrophoretic separation of proteins on microchips," *J. Microcol. Sep.* 12, 407-411.

16. Henry, A. C., Tutt, T. J., Galloway, M., Davidson, Y. Y., McWhorter, C. S., Soper, S. A., and McCarley, R. L. (2000). "Surface modification of poly(methyl methacrylate) used in the fabrication of microanalytical devices," *Anal. Chem.* 72, 5331-5337.

17. Li, J., Thibault, P., Bings, N. H., Skinner, C. D., Wang, C., Coyler, C., and Harrison, J. (1999). "Integration of microfabricated devices to capillary electrophoresis-electrospray ionization mass spectrometry using a low dead volume connection, application to rapid analysis of proteolytic digests," *Anal. Chem.* 71, 3036-3045.

18. Lichtenberg, J., Verpoorte, E., de Rooij, N. F. (2001). "Sample preconcentration by field amplification stacking for microchip-based capillary electrophoresis," *Electrophoresis* 22, 258-271.

19. Kaniansky, D., Masar, M., Bielcikova, J., Ivanyi, F., Eisenbeiss, F., Stanislawski, B., Grass, B., Neyer, A., and Johnck, M. (2000). "Capillary electrophoresis separations on a planar chip with the column-coupling configuration of the separation channels," *Anal. Chem.* 72, 3596-3604.

20. Wainright, A., Williams, S. J., Ciambrone, G., Xue, Q., Wei, J., and Harris, D. (2002). "Sample preconcentration by isotachophoresis in microfluidic devices," *J. Chromatogr. A* 979, 69-80.

21. Figeys, D., and Aebersold, R. (1998). "Nanoflow solvent gradient delivery from a microfabricated device for protein identifications by electrospray ionization mass spectrometry," *Anal. Chem.* 70, 3721-3727.

22. Hofmann, O., Che, D., Cruickshank, K. A., and Müller, U. R. (1999). "Adaptation of capillary isoelectric focusing to microchannels on a glass chip," *Anal. Chem.* 71, 678-686.

23. Rossier, J. S., Schwarz, A., Reymond, F., Ferrigno, R., Bianchi, F., and Girault, H. H. (1999). “Microchannel networks for electrophoretic separations,” *Electrophoresis* 20, 727-731.

24. Mao, Q., and Pawliszyn, J. (1999). “Demonstration of isoelectric focusing on an etched quartz chip with UV absorption imaging detection,” *Analyst* 124, 637–641.

25. Wen, J., Lin, Y., Xiang, F., Matson, D. W., Udseth, H. R., and Smith, R. D. (2000). “Microfabricated isoelectric focusing device for direct electrospray ionization-mass spectrometry,” *Electrophoresis* 21, 191-197.

26. Chen, X., Wu, H., Mao, C., and Whitesides, G. M. (2002). “A prototype two-dimensional capillary electrophoresis system fabricated in poly(dimethylsiloxane),” *Anal. Chem.* 74, 1772-1778.

27. Herr, A. E., Molho, J. I., Drouvalakis, K.A., Mikkelsen, J. C., Utz, P. J., Santiago, J. G., and Kenny, T. W. (2003). “On-chip coupling of isoelectric focusing and free solution electrophoresis for multidimensional separations,” *Anal. Chem.* 75, 1180-1187.

28. Yao, S., Anex, D. S., Caldwell, W. B., Arnold, D. W., Smith, K. B., and Schultz, P. G. (1999). “SDS capillary gel electrophoresis of proteins in microfabricated channels,” *Proc. Natl. Acad. Sci. USA* 96, 5372-5377.

29. Liu, Y. J., Foote, R. S., Jacobson, S. C., Ramsey, R. S., and Ramsey, J. M. (2000). “Electrophoretic separation of proteins on a microchip with noncovalent postcolumn labeling,” *Anal. Chem.* 72, 4608-4613.

30. Bousse, L., Mouradian, S., Minalla, A., Yee, H., Williams, K., and Dubrow, R. (2001). “Protein sizing on a microchip,” *Anal. Chem.* 73, 1207-1212.

31. Benedek, K., and Guttman, A. (1994). “Ultra-fast high-performance capillary sodium dodecyl sulfate gel electrophoresis of proteins,” *J. Chromatogr. A* 680, 375-381.

32. Giddings, J. C. (1991) *Unified Separation Science*, John Wiley & Sons, New York.

33. Rocklin, R. D., Ramsey, R. S., and Ramsey, J. M. (2000). “A microfabricated fluidic device for performing two-dimensional liquid-phase separations,” *Anal. Chem.* 72, 5244-5249.

34. Gottschlich, N., Jacobson, S. C., Culbertson, C. T., and Ramsey, J. M. (2001). “Two-dimensional electrochromatography/capillary electrophoresis on a microchip,” *Anal. Chem.* 73, 2669-2674.

35. Becker, H., Lowack, K., and Manz, A. (1998). “Planar quartz chips with submicron channels for two-dimensional capillary electrophoresis applications,” *J. Micromech. Microeng.* 8, 24-28.

36. Nelson, D. L., Cox, M. M., (2000) *Lehninger Principles of Biochemistry*, Worth Publishers, New York

37. Conn, E. E., Stumpf, P. K., (1976) *Outlines of Biochemistry*, John Wiley & Sons, New York

38. Cunningham, E. B., (1980) *Biochemistry: Mechanisms of Metabolism*, McGraw-Hill Book Company

39. Fruton, J. S., (1999) *Proteins, Enzymes, Genes: the Interplay of Chemistry and Biology*, Yale University Press, New Haven and London

40. Mazur, A., Harrow, B., (1971) *Textbook of Biochemistry*, W. B. Saunders Company

41. Rodriguez-Diaz, R., Wehr, T., Zhu, M., Levi, V., (1997) “Capillary Isoelectric Focusing”, in “*Handbook of Capillary Electrophoresis*” (Landers, J. P. ed.), CRC Press, pp. 101-139.

42. Mohan, D., Lee, C. S., (2002) “Extension of Separation Range in Capillary Isoelectric Focusing for Resolving Highly Basic Biomolecules”, *J. Chromatogr. A*, 979, 271-276.

43. Conti, M., Gelfi, C., and Righetti, P. G. (1996). “Screening of umbilical cord blood hemoglobins by isoelectric focusing in capillaries,” *Electrophoresis* 16, 1485-1491.

44. Conti, M., Galassi, M., Bossi, A., Righetti, P. G., (1997) “Capillary Isoelectric Focusing: the Problem of Protein Solubility”, *J. Chromatogr. A*, 757, 237-245.

45. Chevallet, M., Santoni, V., Poinas, A., Rouquie, D., Fuchs, A., Kieffer, S., Rossignol, M., Lunardi, J., Garin, J., Rabilloud, T., (1998) “New Zwitterionic Detergents Improve the Analysis of Membrane Proteins by Two-Dimensional Electrophoresis”, *Electrophoresis*, 19, 1901.

46. Pedersen, S. K., Harry, J. L., Sebastian, L., Baker, J., Traini, M. D., McCarthy, J. T., Manoharan, A., Wilkins, M. R., Gooley, A. A., Righetti, P. G., Packer, N. H., Williams, K. L., Herbert, B. R., (2003) “Unseen Proteome: Mining Below the Tip of the Iceberg to Find Low Abundance and Membrane Proteins”, *J. Prot. Res.*, 2, 303.

47. Macounova, K., Cabrera, C. R., Holl, M. R., and Yager, P. (2000). “Generation of Natural pH Gradients in Microfluidic Channels for Use in Isoelectric Focusing,” *Anal. Chem.* 72, 3745-3751.

48. Macounova, K., Carbrera, C. R., Yager, P., (2001) “Concentration and Separation of Proteins in Microfluidic Channels on the Basis of Transverse IEF”, *Anal. Chem.*, 73, 1627.

49. Li, Y., DeVoe, D. L., and Lee, C. S. (2003). “Dynamic Analyte Introduction and Focusing in Plastic Microfluidic Devices for Proteomic Analysis,” *Electrophoresis* 24, 193-199.

50. Ofarrell, P. H., (1985) “Separation Techniques Based on the Opposition of Two Counteracting Forces to Produce a Dynamic Equilibrium”, *Science*, 227, 1586.

51. Koegler, W. S., Ivory, C. F., (1996) “Focusing Proteins in an Electric Field Gradient”, *J. Chromatogr A*, 726, 229-236.

52. Ross, D., and Locascio, L. E. (2002). “Microfluidic Temperature Gradient Focusing,” *Anal. Chem.* 74, 2556-2564.

53. Brandt, S., Goffe, R. A., Kessler, S. B., O'Connor, J. L., and Zale, S. E. (1988). “Membrane-based affinity technology for commercial scale purifications,” *Biotechnol.* 6 779-782.

54. Gerstner, J. A., Hamilton, R. S., and Cramer, M. J. (1992). “Chromatographic membrane systems for high throughput gradient separations of biomolecules,” *J. Chromatogr.* 569, 173-180.

55. Roper, D. K., Lightfoot, E. N. (1995). “Separation of biomolecules using adsorptive membranes,” *J. Chromatogr. A* 702, 3-26.

56. Tennikova, T. B., and Svec, F. (1993). “High-performance membrane chromatography: Highly efficient separation method for proteins in ion-exchange, hydrophobic interaction and reversed-phase modes,” *J. Chromatogr.* 646, 279-288.

57. Giovannini, R., Freitag, R., and Tennikova, T. B. (1998). “High-Performance Membrane Chromatography of Supercoiled Plasmid DNA,” *Anal. Chem.* 70, 3348-3354.

58. Podgornik, A., Barut, M., Jan□ar, J., Štrancar, A., and Tennikova, T. (1999). “High-Performance Membrane Chromatography of Small Molecules,” *Anal. Chem.* 71, 2986-2991.

59. Podgornik, A., Barnut, M., Jan□ar, J., and Štrancar, A. (1999). “Isocratic separations on thin glycidyl methacrylate-ethylenedimethacrylate monoliths,” *J. Chromatogr. A* 848, 51-60.

60. Iwata, H., Saito, K., Furusaki, S., Sugo, T., and Okamoto, J. (1991). “Adsorption Characteristics of an Immobilized Metal Affinity Membrane,” *Biotechnol. Prog.* 7, 412-418.

61. Nakamura, M., Kiyohara, S., Saito, K., Sugita, K., and Sugo, T. (1999). “High Resolution of DL-Tryptophan at High Flow Rates Using a Bovine Serum Albumin-Multilayered Porous Hollow-Fiber Membrane,” *Anal. Chem.* 71, 1323-1325.

62. Nakamura, M., Kiyohara, S., Saito, K., Sugita, K., and Sugo, T. (1998). “Chiral separation of DL-tryptophan using porous membranes containing multilayered bovine serum albumin crosslinked with glutaraldehyde,” *J. Chromatogr. A* 822, 53-58.

63. Josic, D., Schwinn, H., Strancar, A., Podgornik, A., Barut, M., Lim, Y.-P., and Vodopivec, M. (1998). “Use of compact, porous units with immobilized ligands with high molecular masses in affinity chromatography and enzymatic conversion of substrates with high and low molecular masses,” *J. Chromatogr. A* 803, 61-71.

64. Xie, S., Svec, F., and Frechet, J. M. J. (1999). “Design of reactive porous polymer supports for high throughput bioreactors: Poly(2-vinyl-4,4-dimethylazlactone-*co*-acrylamide-*co*-ethylene dimethacrylate) monoliths,” *Biotech. & Bioeng.* 62, 30-35.

65. Jiang, Y., and Lee, C. S. (2001). “On-line coupling of micro-enzyme reactor with micro-membrane chromatography for protein digestion, peptide separation, and protein identification using electrospray ionization mass spectrometry,” *J. Chromatogr. A* 924, 315-322.

66. Wang, P.-C., Gao, J., and Lee, C. S. (2002). “High-resolution chiral separation using microfluidics-based membrane chromatography,” *J. Chromatogr. A* 942, 115-122.

67. Cooper, J. W., Chen, J., Li, Y., and Lee, C. S. (2002) submitted to *Anal. Chem.* for publication.

68. Tang, Q., Harrata, A. K., and Lee, C. S. (1995). “Capillary Isoelectric Focusing-Electrospray Mass Spectrometry for Protein Analysis,” *Anal. Chem.* 67, 3515-3519.

69. Tang, Q., Harrata, A. K., and Lee, C. S. (1996). “High-Resolution Capillary Isoelectric Focusing-Electrospray Ionization Mass Spectrometry for Hemoglobin Variants Analysis,” *Anal. Chem.* 68, 2482-2487.

70. Lutkemeyer, D., Bretschneider, M., Buntemeyer, H., and Lehmann, J. (1993). “Membrane chromatography for rapid purification of recombinant antithrombin III and monoclonal antibodies from cell culture supernatant,” *J. Chromatogr.* 639, 57-66.

71. Dubinina, N. I., Kurenbin, O. I., and Tennikova, T. B. (1996). “Peculiarities of gradient ion-exchange high-performance liquid chromatography of proteins,” *J. Chromatogr. A* 753, 217-225.

72. Tennikov, M. B., Gazdina, N. V., Tennikova, T. B., and Svec, T. (1998). “Effect of porous structure of macroporous polymer supports on resolution in high-performance membrane chromatography of proteins,” *J. Chromatogr. A* 798, 55-64.

73. Zeng, X., and Ruckenstein, E. (1999). “Membrane Chromatography: Preparation and Applications to Protein Separation,” *Biotech. Prog.* 15, 1003-1019.

74. Woolley, A. T., Hadley, D., Landre, P., deMello, A. J., Mathies, R. A., and Northrup, M. A. (1996). “Functional Integration of PCR Amplification and Capillary Electrophoresis in a Microfabricated DNA Analysis Device,” *Anal. Chem.* 68, 4081-4086.

75. McCormick, R. M., Nelson, R. J., Alonso-Amigo, M. G., Benvegnu, D. J., and Hooper, H. H. (1997). “Microchannel Electrophoretic Separations of DNA in Injection-Molded Plastic Substrates,” *Anal. Chem.* 69, 2626-2630.

76. Schmalzing, D., Adourian, A., Koutny, L., Ziaugra, L., Matsudaira, P., and Ehrlich, D. (1998). “DNA Sequencing on Microfabricated Electrophoretic Devices,” *Anal. Chem.* 70, 2303-2310.

77. Fan, Z. H., Mangru, S., Granzow, R., Heaney, P., Ho, W., Dong, Q., and Kumar, R. (1999). “Dynamic DNA Hybridization on a Chip Using Paramagnetic Beads,” *Anal. Chem.* 71, 4851-4859.

78. Guttman, A., and Khandurina, J. (2000). “Bioanalysis in microfluidic devices,” *J. Chromatogr. A* 943, 159-183.

79. Foquet, M., Korlach, J., Zipfel, W., Webb, W. W., and Craighead, H. G. (2002) “DNA Fragment Sizing by Single Molecule Detection in Submicrometer-Sized Closed Fluidic Channels,” *Anal. Chem.* 74, 1415-1422.

80. Boone, T. D., Fan, Z. H., Hooper, H. H., Ricco, A. J., Tan, H., and Williams, S. J. (2002). “Plastic Advances Microfluidic Devices” *Anal. Chem.* 74, 78A-86A.

81. Chiem, N., and Harrison, D. J., (1997). “Microchip-Based Capillary Electrophoresis for Immunoassays: Analysis of Monoclonal Antibodies and Theophylline,” *Anal. Chem.* 69, 373-378.

82. Wang, J., Chatrathi, M. P., and Tian, B. (2000). “Micromachined Separation Chips with a Precolumn Reactor and End-Column Electrochemical Detector,” *Anal. Chem.* 72, 5774-5778.

83. Zugel, S. A., Burke, B. J., Regnier, F. E., and Lytle, F. E. (2000). “Electrophoretically Mediated Microanalysis of Leucine Aminopeptidase Using Two-Photon Excited Fluorescence Detection on a Microchip,” *Anal. Chem.* 72, 5731-5735.

84. Dodge, A., Fluri, K., Verpoorte, E., and de Rooij, N. F. (2001). “Electrokinetically Driven Microfluidic Chips with Surface-Modified Chambers for Heterogeneous Immunoassays,” *Anal. Chem.* 73, 3400-3409.

85. Herr, A. E., Molho, J. I., Santiago, J. G., Kenny, T. W., Borkholder, D. A., Kintz, G. J., Belgrader, P., and Northrup, M. A. (2001). “Microchip isoelectric focusing using a miniature scanning detection system,” *Electrophoresis* 22, 2291-2295.

86. Rodriguez-Diaz, R., Wehr, T., Zhu, M., and Levi, V. (1997). “Capillary Isoelectric Focusing,” in “*Handbook of Capillary Electrophoresis*” (Landers, J. P. ed.), CRC Press, pp. 101.

87. Tang, Q., and Lee, C. S. (1997). “Effects of electroosmotic flow on zone mobilization in capillary isoelectric focusing,” *J. Chromatogr. A* 1997, 781, 113-118.

88. Jackman, R. J., Duffy, D. C., Ostuni, E., Willmore, N. D., and Whitesides, G. M. (1998). “Fabricating Large Arrays of Microwells with Arbitrary Dimensions and Filling Them Using Discontinuous Dewetting,” *Anal. Chem.* 70, 2280-2287.

89. Hjerten, S., and Zhu, M. D., (1985). “Adaptation of the equipment for high-performance electrophoresis to isoelectric focusing,” *J. Chromatogr.* 346, 265-270.

90. Hjerten, S., Elenbring, K., Kilar, F., Liao, J. L., Chen, A. J. C., Siebert, C. J., and Zhu, M. D. (1987) “Carrier-free zone electrophoresis, displacement electrophoresis and isoelectric focusing in a high-performance electrophoresis apparatus,” *J. Chromatogr.* 403, 47-61.

91. Richards, D. P., Stathakis, C., Polakowski, R., Ahmadzadeh, H., and Dovichi, N. J. (1999). “Labeling effects on the isoelectric point of green fluorescent protein,” *J. Chromatogr. A* 853, 21-25.

92. Jungblut, P., Thiede, B., Zimny-Arndt, U., Muller, E.-C., Scheler, C., Wittmann-Liebold, B., and Otto, A. (1996). “Resolution power of two-dimensional electrophoresis and identification of proteins from gels,” *Electrophoresis* 17, 839-847.

93. Steinberg, T. H., Haugland, R. P., and Singer, V. L. (1996). “Applications of SYPRO Orange and SYPRO Red Protein Gel Stains,” *Anal. Biochem.* 239, 238-245.

94. Wu, X.-Z., Sze, N. S.-K., and Pawliszyn, J. (2001). “Miniaturization of capillary isoelectric focusing,” *Electrophoresis* 22, 3968-3971.

95. Tan, W., Fan, Z. H., Qiu, C. X., Ricco, A. J., and Gibbons, I. (2002). “Miniaturized capillary isoelectric focusing in plastic microfluidic devices,” *Electrophoresis* 23, 3638-3645.

96. Csapo, Z., Gerstner, A., Sasvari-Szekely, M., and Guttman, A. (2000). “Automated Ultra-Thin-Layer SDS Gel Electrophoresis of Proteins Using Noncovalent Fluorescent Labeling,” *Anal. Chem.* 72, 2519-2525.

97. Yan, J. X., Harry, R. A., Spibey, C., and Dunn, M. J. (2000). “Postelectrophoretic staining of proteins separated by two-dimensional gel electrophoresis using SYPRO dyes,” *Electrophoresis* 21, 3657-3665.

98. Lopez, M. F., Berggren, K., Chernokalakaya, E., Lazarev, A., Robinson, M., and Patton, W. F. (2000) “A comparison of silver stain and SYPRO Ruby Protein Gel Stain with respect to protein detection in two-dimensional gels and identification by peptide mass profiling,” *Electrophoresis* 21, 3673-3683.

99. Berggren, K., Chernokalskaya, E., Steinberg, T. H., Kemper, C., Lopez, M. F., Diwu, Z., Haugland, R. P., and Patton, W. F. (2000) “Background-free, high sensitivity staining of proteins in one- and two-dimensional sodium dodecyl sulfate-polyacrylamide gels using a luminescent ruthenium complex,” *Electrophoresis* 21, 2509-2521.

100. Huang, Z., Munro, N., Huhmer, A. F., and Landers, J. P. (1999). “Acousto-Optical Deflection-Based Laser Beam Scanning for Fluorescence Detection on Multichannel Electrophoretic Microchips,” *Anal. Chem.* 71, 5309-5314.

101. Emrich, C. A., Tian, H., Medintz, I. L., and Mathies, R. A. (2002). “Microfabricated 384-Lane Capillary Array Electrophoresis Bioanalyzer for Ultrahigh-Throughput Genetic Analysis,” *Anal. Chem.* 74, 5076-5083.